A STUDY OF ELECTRONIC ANALOGUE COMPUTERS AND THEIR APPLICATION TO PROBLEMS IN ELECTRICAL ENGINEERING.

A Thesis presented to the
Department of Electrical Engineering
of the University of the Witwatersrand
in partial fulfilment of the requirements
for the degree of Master of Science in Engineering

R. Hemp

August 1971

SUMMARY

The main subject of this dissertation is the investigation of the performance of a position control servomechanism with both torque limitation and integral of error control. The effects of viscous friction were included. The performance of the servomechanism in the linear regime was investigated using the root locus method, while non-linear performance was investigated on an analogue computer.

The introduction (section 1) contains a short description of the importance of methods for the analysis of non-linear systems and mentions the use of both phase - plane techniques and an analogue computer for the investigation of non-linear systems.

Section 2 covers different aspects of the operation of analogue computers. This section does not attempt to provide a comprehensive description of analogue computers, but rather tends to highlight general principles and those aspects of computer operation which were of importance in the subsequent work on the servomechanism.

Section 2.1 is a general description of analogue computers, and distinguishes between differential analysers and dynamic analogies.

The linear operation of the analogue computer is considered in section 2.2. This section starts with the operational amplifier. General equations describing the operational amplifier are given in 2.21, while section 2.211 contains information on such amplifier characteristics as open loop gain, drift and input and output impedances. Both vacuum tube and solid state amplifiers are covered. Sections 2.212 and 2.213 deal briefly with the operation of the inverting and integrating circuits.

Sections 2.22 and 2.23 contain descriptions of the properties of those input and feedback components which were used in the work on the analogue. Polystyrene capacitors were used, and sections 2.221 and 2.222 contain a survey of the literature on the properties of this dielectric. The important point is made that for polystyrene it is not sufficient to consider the capacitor as a simple series or parallel combination of pure resistance and capacitance. As the loss tangent remains constant the series or parallel resistor would have to have a value dependent on frequency. The stability and temperature coefficient of cracked carbon resistors are described in 2.231 and 2.232, while non-

.../linearity

linearity and the effects of frequency are covered in 2.233 and 2.234.

Section 2.3 covers the use of diodes for the simulation of saturation non-linearities on the analogue computer.

The description of the analogue computer is concluded with a section on scaling. A method of estimating maximum values of system variables is described briefly.

Section 3 deals with the position control servomechanism, and starts with a short survey of previous work in this field. Section 3.2 deals with the linear analysis of the servomechanism. Basic equations are derived (section 3.21) and these are manipulated to obtain suitable equations for the plotting of root loci. In this instance the root loci are not true loci and only have a physical meaning at the closed loop poles. Investigation of the equations with a view to normalisation (section 3.22) shows that this is not possible in a convenient form. In section 3.23 the conditions for which root loci were drawn are listed, and the calculation of step function responses from closed loop pole positions described briefly.

Section 3.3 covers the use of the analogue computer to investigate operation in the non-linear regime. All the computer results are presented graphically as step function responses. Results for linear operation were compared with calculated figures, and were, with one exception, found to agree reasonably well.

The appendices (section 6) contain firstly (section 6.1) some measurements on the non-linearity of some actual servomechanism components. It is concluded that the use of diodes for the simulation of non-linearity is satisfactory. Section 6.2 describes the measurement of the input and feedback components which were used on the analogue. The use of a simple oscillator circuit to check these measured values is described in 6.23. The final section (6.3) gives the results of measurements of the pen recorder characteristics.

CONTENTS

1. INTRODUCTION

While early work on servomechanism theory was confined largely to methods of analysis and synthesis of linear systems, the analysis of non-linear systems has become increasingly important. Section 3.1 of this dissertation contains a description of investigations which have been carried out into the performance of remote position control servomechanisms with various non-linearities, and it is apparent from this that the non-linear behaviour of this particular servomechanism has received considerable attention.

West, Douce and Naylor[1] and West and Nikiforuk[4] have both emphasised that the presence of non-linearities is not necessarily undesirable, and in fact can be made into a desirable feature of a servomechanism. This can only be achieved however, through an understanding of the characteristics of non-linear systems. West[5] has pointed out the many difficulties which arise in the analysis of non-linear systems, and has provided a comprehensive description of the various analytical techniques available for this task. In addition he emphasises that saturation non-linearities exist in every servomechanism, and will modify the performance of the system to a greater or lesser degree.

The analysis of non-linear servomechanisms is usually confined to the determination of the transient response, normally the step-function response. Both Holt-Smith[2] and Coales[3] in a contribution to the paper by West, Douce and Naylor[1] have made the point that while for a linear system knowledge of either the transient response or the frequency response is, in theory, sufficient for a full knowledge of the servomechanism performance, the same does not necessarily hold for a non-linear system. In their reply to discussion the authors agree with this, but defend their use of the step-function response by pointing out that knowledge of this response is on its own of value. Tustin[7], in a contribution to a paper by West and Nikiforuk[6], makes the same point when he queries the practical value of evaluating the step-function response. Once again, the authors agree, and while they feel that the random

.../input

input response will prove of more value, they nevertheless think that the evaluation of step-function response will lead to a better understanding of the performance of the non-linear system, and a better assessment of its adequacy for a given set of requirements.

The most common method for the analysis of non-linear systems is perhaps the phase-plane. The use of this method is described in most textbooks on servomechanism theory. Good descriptions are given by, for example, Hammond[8], Thaler and Pastel[9], Truxal[10], and West[5]. West has pointed out that while the phase-plane method can be applied to many problems by a suitable transformation of variables the method has most meaning when the variables are velocity and position, for these are easily visualised. In general the phase-plane method is restricted to the transient analysis of systems of second-order which are subjected to initial conditions only, and are not otherwise excited. Kalman[11], however, has extended and generalised the method to systems governed by higher-order non-linear differential equations.

Analogue computers are commonly used for the analysis of non-linear servomechanism performance. Most published work deals with the use of analogue computers for the determination of the transient response of the system, but the analogue computer is obviously not limited in this regard. West and Nikiforuk[4,6], for example, in two papers describe the use of the analogue computer for the determination of both the frequency response and the response to random inputs of a non-linear remote position control servomechanism. Douce and King[12] also used the analogue computer to determine, again for a non-linear system, the response to both sinusoidal and Gaussian noise inputs.

2. THE ANALOGUE COMPUTER

2.1 GENERAL

Both Hammond[8] and Paul[13] draw a clear distinction between differential analysers and dynamic analogies. Paul described a dynamic analogy as a representation of one physical model by another model of a different physical form, both models having their dynamic performance described by identical mathematical relationships. The obvious and often quoted example is the analogy between electrical circuits containing resistance, inductance and capacitance and mechanical systems with both energy storage (e.g. in a flywheel or spring) and friction.

A differential analyser on the other hand, as its name implies, provides the means for the solution of the differential equations describing the operation of a system. This is accomplished by the suitable interconnection of components which perform such operations as differentiation, integration, addition, multiplication by a constant, and for non-linear equations multiplication and division. These components are generally complex, and cannot be considered direct analogies of any part of the system under study.

Early differential analysers were mechanical, but these have been completely superceded by electronic analysers, and the term electronic analogue computer is generally taken to refer to an electronic differential analyser. This dissertation will be confined to electronic differential analysers or analogue computers. The principle of operation of an electronic analogue computer is well known, and has been described in publications such as Hammond[8], Paul[13], Harris[14], Levine[15], Pfeffer[16], Korn and Korn[17] and Jackson[18]. In this dissertation various specific aspects of analogue computer operation are investigated.

The heart of the electronic analogue computer is the operational amplifier. This is a high negative gain d.c. amplifier which is used with passive input and feedback components to provide the desired transfer function. Early operational

.../amplifiers

amplifiers were, naturally enough, vacuum tube amplifiers. Within the last decade, however, the use of solid state amplifiers has increased considerably. Vacuum tube amplifiers have the advantage of being able to operate at output voltage levels about an order of magnitude higher than solid state amplifiers.

Section 2.21 contains a detailed analysis of the performance of an operational amplifier when input and feedback impedances are connected. This analysis shows the major role played by input and feedback impedances in determining the transfer function of the circuit. These input and feedback impedances can be thought of as defining the mathematical operations performed by the operational amplifier. Harris[14] has listed two sources of error in an operational amplifier :-

i. the accuracy and stability of the electrical networks defining the mathematical operations to be performed

ii. the presence of any voltage signals in the system other than those corresponding to the problem variables.

If the network defining the mathematical operations is taken to be the input and feedback impedances only, a further error source can be added to the above list, viz. the effect of the departures from ideal amplifier performance upon the operation of the circuit.

These three sources of error are considered further in the following sections.

Pfeffer[16] has given some useful general information on errors in electronic analogue computers. Potentiometer errors resulting from such factors as inaccuracy in voltmeters, resolution and stability can be as low as 0,01 to 0,02%. Similarly, the use of high quality input and feedback impedances and the housing of these in a temperature controlled oven leads to feedback ratios accurate to within 0,01 or 0,02%. Amplifier gains are usually sufficiently high to cause the error in closed loop gain to be

.../considerably

considerably less than 0,01%. Loading errors are also generally very low indeed. Recorders, especially when small numbers of operational amplifiers are used, restrict the overall accuracy. Galvanometer recorders are generally only accurate to within 2 to 5%, and while servo-type recorders have a considerably higher accuracy (0,1 to 0,5%) they do have the disadvantage of a severely limited maximum frequency, usually less than 1 Hz (see also section 2.4).

2.2 LINEAR OPERATION

2.21 The Operational Amplifier

Figure 2.1 shows an operational amplifier with feedback impedance and several inputs, each connected to the amplifier through a separate input impedance.

Korn and Korn[17] have given the following expression for the output voltage e_o in terms of the input voltages e_{ik}, the input and feedback impedances and the gain of the amplifier. The input impedance of the amplifier is assumed to be infinite and the output impedance zero.

$$e_o = -(1 - \frac{1}{1-A\beta}) \, (e_{i1} \frac{Z_f}{Z_{i1}} + e_{i2} \frac{Z_f}{Z_{i2}} + \text{-----} + e_{ik} \frac{Z_f}{Z_{ik}}) \qquad (1)$$

$$\text{where } \beta = (1 + \frac{Z_f}{Z_{i1}} + \frac{Z_f}{Z_{i2}} + \text{-----} + \frac{Z_f}{Z_{ik}})^{-1}$$

Both A, the amplifier gain (negative and real at low frequencies), and β are functions of frequency. The feedback circuit is obviously stable if, and only if, all roots of the characteristic equation $1 - A(s)\beta(s)$ have negative real parts.

Stability of the circuit is generally achieved by proper design of the gain characteristic of the operational amplifier. The components necessary for this frequency compensation are generally incorporated in the amplifier for vacuum tube amplifiers

.../and

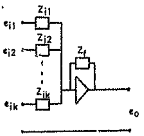

FIGURE 2-1

and discrete component solid state amplifiers. However the capacitors are usually orders of magnitude larger than can be fabricated by monolithic techniques, and as a result integrated circuit operational amplifiers usually require external frequency compensation[19,20].

When the amplifier is inverting (i.e. it has negative gain), and the gain A is very high

$$e_o \doteq -(e_{i1} \frac{Z_f}{Z_{i1}} + e_{i2} \frac{Z_f}{Z_{i2}} + \text{----} + e_{ik} \frac{Z_f}{Z_{ik}})$$

The output of the operational amplifier is thus the sum of functions of the input voltages, the form of the function's depending on the input and feedback impedances only. An operational amplifier with only a single input has its output voltage given by

$$e_o = -e_i \frac{Z_f}{Z_i}$$

When both input and output impedances are resistors, $Z_f = R_f$ and $Z_i = R_i$.

$$e_o = -e_i \frac{R_f}{R_i}$$

and the operational amplifier multiplies the input voltage by a negative constant $-\frac{R_f}{R_i}$.

When the feedback impedance is a capacitor and the input impedance a resistor, $Z_f = \frac{1}{sC}$, $Z_i = R_i$

$$e_o = -e_i \frac{1}{sR_iC} = -\frac{1}{R_iC} \int e_i \quad dt$$

and the operational amplifier operates as an integrator with time constant R_iC.

.../Equation

Equation 1 derived by Korn and Korn[17] only applies when the amplifier has infinite input impedance and zero output impedance. They have also considered the situation when these two restrictions do not apply.

When the load connected to the output of the operational amplifier has an impedance Z_L, and the amplifier an output impedance Z_o the effective amplifier forward gain A is given by

$$A = \frac{A_o + \frac{Z_o}{Z_f}}{1 + \frac{Z_o}{Z_f} + \frac{Z_o}{Z_L}} \qquad \text{---(2)}$$

where A_o is the open circuit gain of the amplifier.

The operation of the complete circuit can be analysed by using Thévenin's theorem. The operational amplifier circuit appears to the load Z_L as a voltage source e_o' in series with an impedance Z_s. The voltage source e_o' is the output voltage of the operational amplifier without load, given by equations (1) and (2) with $Z_L \longrightarrow \infty$

and $A = \dfrac{A_o + \frac{Z_o}{Z_f}}{1 + \frac{Z_o}{Z_f}}$

The series impedance Z_s is given by

$$Z_s = \frac{Z_f \ Z_o}{(1 - \beta)\ Z_o + (1 - A_o\beta)\ Z_f}$$

$$Z_s \doteqdot - \frac{Z_o}{A_o\beta} \text{ when } \left|A_o\beta\right| \gg 1$$

The total output voltage e_o of the operational amplifier is then given by

.../ e_o

$$e_o = \frac{Z_L}{Z_s + Z_L} \quad e_o'$$

The effect of the amplifier input impedance can be obtained by considering the amplifier input impedance as the input impedance associated with an additional voltage source. The voltage source is of course zero. If the amplifier input impedance is Z_a equation (1) becomes

$$e_o = -(1 - \frac{1}{1 - A\beta}) (e_{i1} \frac{Z_f}{Z_{i1}} + e_{i2} \frac{Z_f}{Z_{i2}} + ---- + e_{ik} \frac{Z_f}{Z_{ik}})$$

where now $\beta = (1 + \frac{Z_f}{Z_{i1}} + \frac{Z_f}{Z_{i2}} + ---- + \frac{Z_f}{Z_{ik}} + \frac{Z_f}{Z_s})^{-1}$

The preceding few pages give a complete description of operational amplifier performance when the output voltage of the d.c. amplifier is given by the product of the gain and the input voltage. This is not generally correct, for all d.c. amplifiers are subject to drift, i.e. the appearance at the output of spurious voltages. Before considering in more detail the operation of the most commonly used operational amplifier configurations some aspects of operational amplifier performance will be investigated.

2.211 Amplifier Drift

As mentioned above the output voltage of a d.c. amplifier is generally not zero when zero input voltage is applied. The application of a voltage offset to the amplifier can ensure zero output voltage. When, however, the magnitude of the voltage offset required for zero output voltage varies with time it is not generally possible to ensure that the amplifier output voltage is given by the product of gain and the input voltage, and drift is present. It

.../is

is customary to refer all voltage offset and drift values to the amplifier input.

There are many causes of drift. Korn and Korn[17] list the following factors which can cause drift in a vacuum tube amplifier.

i. changes in supply voltages
ii. changes in resistance values
iii. changes in vacuum tube characteristics.

Drift in solid state operational amplifiers results from the variation of both voltage and current offset.

Pearlman[19] points out that the stability of the voltage offset in a solid state amplifier depends on the degree to which the pair of input transistors can be matched and will track with temperature. Stata[21] emphasises the important effect of temperature. The base-emitter voltage of a transistor varies at approximately 2 400 uV/^{o}C. The use of matched pairs can result in net changes of about 5 uV/^{o}C when the two transistors are at equal temperatures. A temperature differential of only 0,01^{o}C however, would lead to an offset of 24 uV, or almost five times the nominal figure. Stata points out that temperature differentials arise not only from the obvious sources such as draughts and the proximity of power dissipating components but also by factors such as variations in amplifier load.

Current offset arises when the base current of the input transistors flows through the input impedances[19]. Markkula[20] has discussed the effects of both current and voltage offsets on the output voltage of an operational amplifier, and has shown how the effects of current offset can be minimised by the selection of external circuit components. Routh[22] points out that the input voltage offset for a particular amplifier is fixed, but the effects of current offset depend on the circuit used. Amplifier voltage offset is predominant for low source resistances, while current offset becomes more important when source resistances

.../are

are high. No necessary relationship exists between voltage and current offsets, not even in regard to polarity[23].

The magnitude of voltage and current offsets in solid state amplifiers and of drift in vacuum tube amplifiers obviously depends to a very large extent on the design of the amplifier. Stata[21] makes the very important point that voltage and current offsets in solid state amplifiers are non-linear functions of temperature. The use of average figures can thus be misleading.

Pearlman[19] quotes voltage offsets of the order of 1 to 10 uV/°C and current offsets of the order of 1 nA/°C for discrete component solid state amplifiers. Inspection of maker's data[23] for solid state amplifiers shows that the change of offset voltage with temperature in the range 10 to 60°C varies from 0,4 uV/°C to 60 uV/°C. Current offset variation with temperature over the same range varies from 0,6 pA/°C to 5 nA/°C. Markkula[20], in giving typical figures for several solid state voltage follower circuits, quotes a voltage offset temperature coefficient of 15 uV/°C for a discrete component circuit and values ranging from 0,6 to 4,5 uV/°C for integrated circuits. Corresponding current offset values were 10 nA/°C and 0,002 to 3 nA/°C.

Voltage and current offsets vary with time (½ hour) to the extent of 1 to 25 uV and 0,01 pA to 20 nA in solid state amplifiers[23].

Korn and Korn[17] quote average drifts for chopper stabilised vacuum tube amplifiers of less than 20 to 200 uV, while Pfeffer[16] reports that good amplifiers (vacuum tube) will have drifts of less than 100 uV. It must be remembered that it is possible to operate vacuum tube amplifiers at much higher voltages (generally ± 100v) than solid state amplifiers (generally ± 10v) and drift voltages must be assessed accordingly.

2.2112 Open Loop Voltage Gain

Once again it is difficult, if not impossible, to quote average figures.

.../For

For solid state amplifiers Markkula[20] gives a figure of 10^4 for a discrete component amplifier and values ranging from 4×10^3 to 4×10^7 for integral circuits. Manufacturer's data[23] shows values ranging from 5×10^3 to 5×10^7.

Korn and Korn[17] give values ranging from 25 to 300×10^6 for stabilised vacuum tube amplifiers.

All these figures are for zero frequency (d.c.).

2.2113 Input Impedances

Pearlman[19] reports input impedances of discrete component solid state amplifiers ranging from several hundred kilohms to several megohms. The development of field effect transistors has made possible the construction of direct coupled operational amplifiers having input impedances in the range of 10^{11} to 10^{14} ohms[19]. Other sources quote figures lying within the above limits.

2.2114 Output Impedance

Korn and Korn[17] state that in general the output impedance of vacuum tube amplifiers varies between 1 000 and 5 000 ohms.

2.212 The Inverter

In this circuit the input and feedback impedances are both resistors, although in a unity gain inverter the use of identical reactive or complex impedances will sometimes improve the frequency response.

Using the terminology of 2.21

$$e'_o = -(1 - \frac{1}{1 - A\beta}) \frac{R_f}{R_i} e_i$$

$$\beta = (1 + \frac{R_f}{R_i} + \frac{R_f}{Z_a})^{-1}$$

.../e_o

$$e_o = \frac{Z_L}{Z_s + Z_L} \quad e_o'$$

$$Z_s = \frac{Z_o}{(1 - \beta)\frac{Z_o}{R_f} + (1 - A_o\beta)}$$

$$A = \frac{A_o + \frac{Z_o}{R_f}}{1 + \frac{Z_o}{R_f}}$$

Inspection of the above equations in the light of the amplifier characteristics will generally allow the following approximations to be made

$$A = A_o$$

$$e_o = e_o'$$

$$\therefore \quad e_o = -(1 - \frac{1}{1 - A_o\beta}) \; \frac{R_f}{R_i} \; e_i$$

$$\beta = (1 + \frac{R_f}{R_i} + \frac{R_f}{Z_a})^{-1}$$

Only when $\frac{R_f}{R_i}$ is very high or the amplifier gain very low, will the term $\frac{1}{1 - A_o\beta}$ generally be of any significance.

Amplifier drift will appear at the output multiplied by the gain $\frac{R_f}{R_i}$, and provided the signal voltage level *is not too* low will generally be insignificant.

.../2.213

2.213 The Integrator

Korn and Korn[17] state that "the design of accurate integrators is a crucial part of the entire computer design".

A general equation describing the performance of most d.c. integrators has been given by Korn and Korn[17]

$$e_o = \frac{bk}{bs + 1} e_i$$

where b is the time constant
and k the gain of the circuit.

(This distinction between gain and time co tant has also been drawn by Pfeffer[16]).

Korn and Korn consider the response of the above system to a unit step input. Under these conditions the output voltage is given by

$$e_o = bk\,(1 - \epsilon^{-t/b}) = kt - \frac{k}{2b}t^2 \pm \text{-----}$$

when $e_o = kt$ true integration has been achieved, and the remaining terms in the expansion of $(1 - \epsilon^{-t/b})$ constitute a measure of the error of the circuit.

If $0 \leq t/b < 1$ the absolute value of the error will be less than or equal to $\frac{k}{2b}\ t^2$.

thus $\left|\text{error}\right| \leq \frac{kt^2}{2b}$

and the maximum percentage error $= 50\,\frac{t}{b}$

This is an extremely useful expression, for it allows integrator time constants to be selected in terms of the maximum permissible error and the maximum computing time.

Korn and Korn[17] analysed the integrating operational amplifier by using eqn (1) to determine the gain and time constant of the circuit.

.../They

They obtained the expressions

$$\text{gain} = k = \frac{A}{(1 - A)\ R_1C}$$

$$\text{and time constant} = b = \frac{(1 - A)\ R_1C}{(1 - A)\ \frac{R_1}{R_L} + 1}$$

where R_L is the resistor in parallel with the capacitor to simulate the losses. In section 2.222 it is shown that this resistor varies with frequency, for it is the loss tangent which remains constant, at least in polystyrene capacitors. The use of a constant resistance value in what is essentially a transient analysis is thus incorrect.

If the above is ignored the expression for maximum percentage error becomes

$$\text{max. percentage error} = 50\ \frac{(1 + A)\ {}^{R}/_{R_L} + 1}{(1 + A)\ R_1C}\ t$$

$$= 50\ t\ \left(\frac{1}{R_LC} + \frac{1}{(1 + A)\ R_1C}\right)$$

Table 2.1 shows that for polystyrene capacitors the time constant R_LC is of the order of 10^6s. For an integrator with a time constant R_1C of 1s the first term in brackets will predominate when the amplifier gain is greater than 10^7, and the second term will predominate for amplifier gains less than 10^5.

Taking the first case (amplifier gain greater than 10^7)

$$\text{max. percent error} = 50\ t\ \frac{1}{R_LC}$$

$$= 50\ t \times 10^{-6} \text{ for a polystyrene capacitor.}$$

Thus after 200 seconds the maximum error is 0.01%.

.../ 2.22

2.22 Capacitor Characteristics

It has been shown in 2.21 that the characteristics of an operational amplifier functioning as an integrator (or differentiator) depend to a very large extent upon the properties of the capacitor used. The losses of the capacitor can have a significant effect upon the transfer function of the operational amplifier, and as a result it is necessary to use low loss capacitors.

Polystyrene is a dielectric with very low losses, and capacitors with polystyrene as a dielectric material are commonly used in analogue computers. As all the experimental work described in this thesis was done with polystyrene capacitors the following collection of dielectric and capacitor properties is confined to polystyrene. The properties are considered under the two headings - dielectric constant and capacitance, and losses.

2.221 Dielectric Constant and Capacitance.

Curtis[24], quoting work by Broens and Müller[25] gives values for the dielectric constant of polystyrene of 2,55 at 0°C and 2,51 at 100°C for frequencies between 0,18 and 316 kHz. Von Hippel[26] reports values of 2,56 at 25°C for frequencies between 10^2 and 10^7 Hz, and 2,54 at 80°C for frequencies from 10^2 to 3×10^9 Hz, while Birks[27] gives a value of 2,55 at 20°C for all frequencies up to 10^{10} Hz.

While there are some discrepancies in the values quoted above, they do indicate that polystyrene has a dielectric constant which is remarkably constant over a very large range in frequency. The temperature coefficient of dielectric constant implied by the above figures is about -150×10^{-6} per °C. Charlton and Shen[28], however, emphasise that the temperature coefficient of capacitance depends not only on the dielectric properties of the material, but also on the thermal expansion coefficients of both dielectric and electrodes, and upon the method of construction.

.../ The

The determination of values for the temperature coefficient of capacitance implies that the capacitance returns to its original value after thermal cycling. This will only occur if the capacitor is properly constructed. Charlton and Shen quote figures for the temperature coefficient of capacitance varying from about -100×10^{-6} per $^{\circ}C$ for a 0,1 uF capacitor to about -170×10^{-6} per $^{\circ}C$ for a 0,0005 uF capacitor. They report that encapsulated capacitors only reach a steady state about 60 days after they have been subjected to a $30^{\circ}C$ temperature change, while unprotected capacitors require about 6 days. This property of polystyrene capacitors obviously makes drift measurements difficult, but Charlton and Shen estimate that drifts of 0,1 % and 0,15% would not be exceeded for unprotected and encapsulated components respectively.

The use of temperature controlled ovens for housing input and feedback components in high quality analogue computers (Harris[14] and Pfeffer[16]) obviously considerably reduces the importance of the temperature coefficient. The work described in this dissertation was done without using any temperature control, but as the accuracy was in any case limited, and as the capacitors were not used at temperatures differing greatly from those at which they were measured, it was not felt necessary to take temperature into account.

Dummer[29] quotes a figure of about 0,5% for the drift that could occur in a polystyrene capacitor, and mentions temperature coefficients of capacitance of up to -200×10^{-6} per $^{\circ}C$. Hartshorn, Parry and Rushton[30] carried out very careful experiments to determine the temperature coefficient of <u>permittivity</u> of polystyrene, and obtained a value of -169×10^{-6} per $^{\circ}C$. It was possible to calculate the coefficient of thermal expansion of polystyrene from this value; this calculated value agreed well with the experimentally determined value of 72×10^{-6} per $^{\circ}C$. It is interesting to note that Hartshorn et al quote a value for the temperature coefficient of <u>capacitance</u> for polystyrene capacitors of -350×10^{-6} per $^{\circ}C$.

.../Table 2.1

2.222 Losses

Losses in a capacitor are usually expressed either in terms of a time constant or in terms of the power factor or loss tangent. For low loss capacitors power factor and loss tangent are to all intents and purposes identical.

Table 2.1 summarises values given in the literature for the losses of polystyrene capacitors. Charlton and Shen[28] have pointed out that the large variation in the values of capacitor time constant supports the view that it is the impurities in the dielectric rather than the molecular structure of the dielectric which give rise to losses.. They state that maximum and minimum values of the time constant can differ from their quoted figures by a factor of about 4. Hartshorn, Parry and Rushton[30] have also emphasised the important effect of impurities.

Dummer[29] has stated that for capacitance values less than about 0,1 uF the construction of the capacitor has a greater effect upon the losses than have the properties of the dielectric.

Both Dummer[29] and Charlton and Shen[28] have pointed out that the power factor is essentially independent of frequency. The implications of this are that the normal equivalent circuits (see for example Dummer[31]) given for practical capacitors must have loss resistances whose values vary with frequency.

Consider for example the simple equivalent circuit where the capacitor losses are represented by a resistor R in parallel with the capacitor C. The capacitor impedance Z is then given by

$$Z = \frac{R \ \frac{1}{jwC}}{R + \frac{1}{jwC}}$$

$$= \frac{1}{jwC} \ \left(\frac{1}{1 + \frac{1}{jwRC}} \right)$$

.../ The

Reference	Power factor or loss tangent	Time Constant "s"	Frequency Hz	Temperature °C	REMARKS
Broens & Müller[25]	<0,001	-	$0,18\times10^3$ to $3,16\times10^5$	up to 100	
Von Hippel[26]	<0,00005	-	10^2	25	
	<0,00005	-	10^4		
	0,00007	-	10^6		
	<0,00001	-	10^8		
	0,00043	-	10^{10}		
	0,0009	-	10^2	80	
	<0,0001	-	10^4		
	<0,0002	-	10^6		
	<0,0003	-	10^8		
	0,00053	-	10^{10}		
Birks[27]	0,0002	-	0 to 10^{10}		
Charlton & Shen[28]	0,0002	-	up to several 10^6	working range	
	-	10^6	-	20	Measured on 0,2 - 1,0uF components 1 minute measurements
	-	$6,3\times10^5$	-	40	
	-	$3,2\times10^5$	-	60	
Dummer[29]	0,0005	-	10^3		
Hartshorn et al[30]	0,0001	-	50		
	0,0003	-	10^6		
	0,0004	-	9×10^9		
Dummer[31]	-	$7,3\times10^5$	-	20	
	-	$3,4\times10^5$	-	40	
	-	$1,2\times10^5$	-	60	

TABLE 2.1

.../2.222

The loss tangent tan δ is given by

$$\tan \delta = \frac{1}{wRC}$$

and hence

$$Z = \frac{1}{jwC} \frac{1}{1 - j \tan \delta} \doteq \frac{1}{jwC} (1 + j \tan \delta) \text{ for small } \tan \delta$$

The use of the second expression, with tan δ constant, is obviously preferable to the use of the first, where R is frequency dependent.

2.23 <u>Resistor Characteristics</u>

Following the section on capacitor characteristics, (2.22) this section will be confined to the characteristics of cracked carbon resistors, for these were the resistors used with the analogue computer.

2.231 <u>Stability</u>

Dummer[32] states that cracked carbon resistors show a failure rate of about 3 per 1 000 after operation under laboratory conditions for 12 months. This failure rate is dependent upon environmental conditions, use in air-conditioned surroundings resulted in lower failure rates, while operation under service conditions of extreme temperature and humidity resulted in somewhat higher failure rates. Maximum reliability is attained when resistors are not subjected to excessive temperature or voltage stresses. Average changes in resistance of less than 2% after climatic and other tests are typical for those resistors that do not fail.

Church[33], quoting work by Braner and Easterday[35], states that for resistors operating at full load at 70°C the mean change

.../of

of value was between 0,5 and 1%, with occasional resistors showing much larger changes. The failure rate was found to be higher with full load d.c. testing than with a.c. testing, and under very humid conditions and light d.c. loading very high failure rates were experienced.

Dummer[32] reports that changes in resistance of 2% and above have occurred after storage for one year at room temperature. This is confirmed by Church[34], who mentions that some cracked carbon resistors show appreciable changes after storage.

These figures certainly provide justification for the general use of high precision wirewound resistors in analogue computers, see for example Harris[14]. In this particular instance however, it was felt that the cracked carbon resistors were adequate. Appendix 6.22 gives details of some of the measurements carried out on the set of resistors. Occasional checks on the resistors failed to reveal any evidence of significant resistance changes occurring during the work.

2.232 Temperature Coefficient

Dummer[32] quotes temperature coefficients varying from $0{,}0004/^{\circ}C$ for low resistance values to $0{,}001/^{\circ}C$ for high resistance values. The temperature coefficient is apparently dependent upon the resistivity of the carbon film. The measurements carried out on the set of resistors (appendix 6.22, table 6.8) are in general agreement with the above figures.

The temperature of the resistor is a function of both the ambient temperature and the power dissipation and the following analysis considers the effect of the temperature coefficient and dissipation constant of resistors upon the operation of the analogue computer. This only really has relevance to the present work. As mentioned in 2.231 it is usual to use temperature controlled ovens for input and feedback

.../impedances

impedances in high quality analogue computers. Under these conditions the only effect to be considered is that of power dissipation. The temperature coefficients of the wire wound resistors used are likely to be considerably lower than those of the cracked carbon resistors used in this work, and it is also likely that resistors of higher power rating will be used. The effect of power dissipation is thus likely to be very much less than in the present instance.

The transfer function of an operational amplifier with input and feedback components has been shown (2.22) to be given by

$$\frac{e_o}{e_i} = -\frac{Z_f}{Z_i} \quad \text{neglecting error terms}$$

For the case when both Z_f and Z_i are resistances

$$\frac{e_o}{e_i} = -\frac{R_f}{R_i}$$

Now $R_f = R_{f_o}\left(1 + \alpha_f\left(T + \frac{P_f}{B_f}\right)\right)$ and

$$R_i = R_{i_o}\left(1 + \alpha_i\left(T + \frac{P_i}{B_i}\right)\right)$$

$$\text{then } \frac{e_o}{e_i} = -\frac{R_{f_o}}{R_{i_o}} \; \frac{1 + \alpha_f\left(T + \frac{P_f}{B_f}\right)}{1 + \alpha_i\left(T + \frac{P_i}{B_i}\right)}$$

$$\frac{e_o}{e_i} \doteq -\frac{R_{f_o}}{R_{i_o}}\left(1 + (\alpha_f - \alpha_i)\,T + \left(\frac{\alpha_f}{B_f}\,\frac{R_{f_o}}{R_{i_o}} - \frac{\alpha_i}{B_i}\right) P_i\right)$$

.../Further

Further consideration of errors is best done by referring to typical c… …nent values. Table 6.8 gives values of α and B for …he 0… …d 1,0 megohm cracked carbon resistors used with the a… …omputer.

Considering firstly the effect of ambient temperature, reference to table 6.8 shows that the maximum difference between individual temperature coefficient values is 370 p.p.m./°C. Ambient temperatures are unlikely to vary by more than … 5°C from the reference value of 20°C, an… so this leads to a possible error in the transfer function of about 0,2%. Voltages in the analogue computer are restricted to about 100 volts peak and table 6.8 shows that values of the ratio $\frac{\alpha}{B}$ vary between 36 and 61 for the 0,1 megohm resistors and 41 and 74 for the 1 megohm resistors. The highest power dissipation occurs when two 0,1 megohm resistors are used to provide a gain of -1; under these circumstances $P_i = P_f = 100$ mW and the maximum error of about 0,25% occurs. The increase in resistor temperature caused by power dissipation is essentially a long term effect. The measured values of B were obtained under steady state conditions, and the change in temperature which occurs when a resistor is subjected to a voltage transient lasting for perhaps 5 or 10 seconds is not …asy to predict. The above reasoning thus applies essentially to steady state operation of the amplifier. It can be seen that the resistors used with the analogue computer were such that accuracies considerably better than 0,5% were possible.

2.233 Frequency

Osborne[36], representing the resistor by a parallel … combination of capacitance and inductive resistance, quotes capacitance values ranging from 0,1 to 0,5 pF. The inductance in series with the resistor varies from 0,018 to 1,23 uH for 0,1 megohm resistors and from 0,04 to 1,8 uH for 1 megohm resistors. These figures indicate that, as the frequency increases, the

.../capacitive

capacitive effect predominates, and that, for a 1 megohm resistor the impedance is likely to be about 1% greater then the resistance at a frequency of 30 kHz. This frequency is high enough for the effect to be negligible in all but high frequency repetitive operation of an analogue computer.

2.234 Non-linearity

There are several methods used for evaluating the non-linearity of resistors. Millard[37] mentions the voltage coefficient, which is obtained by measuring the resistance at the maximum voltage (maximum here meaning the highest voltage which can be applied to the resistor without exceeding either the voltage limitation or the maximum power dissipation) and at one tenth of the maximum voltage, care being taken to avoid temperature effects. Dummer[32] quotes values of the voltage coefficient of less than 0,002% per volt.

Both Millard[37] and Kirby[38] assess the non-linearity by measuring the third harmonic voltage arising from the application of the fundamental to the resistor. Millard plots the third harmonic voltage (frequency 3,18 kHz) against the applied fundamental voltage (frequency 1,06 kHz). Typical values obtained on two different low value resistors (50 - 100 ohms) were i) 5×10^{-6} volts at 2 volts and $2,5 \times 10^{-4}$ volts at 7 volts and ii) 2×10^{-6} volts at 4 volts and $1,5 \times 10^{-5}$ volts at 7 volts. Kirby has pointed out that provided the power dissipation is not raised above the nominal value the third harmonic voltage is proportional to the cube of the applied voltage. He defines a logarithmic "third harmonic index" (T.H.I.) as follows

$$\text{T.H.I.} = 20 \log_{10} \frac{\text{r.m.s. uV of third harmonic}}{(\text{r.m.s. volts of applied fundamental})^3}$$

.../and

and gives the following values of the T.H.I. for ½ watt resistors

0,1 megohm	T.H.I. from - 50 to - 80
1 megohm	T.H.I. from - 60 to - 75

It would appear that non-linearity is not a serious problem when cracked carbon resistors are used with the analogue computer.

2.3 SIMULATION OF SATURATION NON-LINEARITIES

Figure 2.2 shows the standard method of using two diodes to simulate a saturation non-linearity. Measurements were made on a circuit having the following nominal transfer function

$$\frac{e_o}{e_i} = -1 \qquad \left|e_i\right| < 0{,}2E$$

$$\left|\frac{e_o}{e_i}\right| = 0{,}2E \qquad \left|e_i\right| > 0{,}2E$$

Figure 2.3 shows the variation of output with input voltage for various values of the diode biasing voltage E.

It is apparent from Figure 2.3 that the shape of the saturation curve depends upon the value of the diode biasing voltage. Figure 2.4 shows the curves given in Figure 2.3 plotted on a scale where both the saturation level and the initial slope are unity. In practice this can be achieved by changing the gains of amplifiers 2 and 4 (Figure 2.2).

.../ Figure 2.2

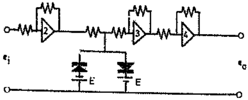

FIGURE 2·2

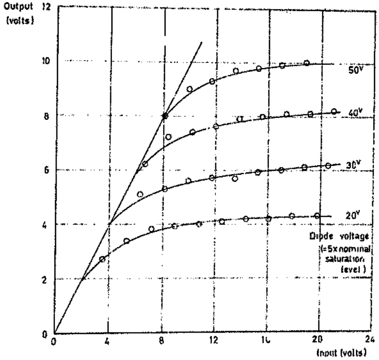

FIGURE 2·3

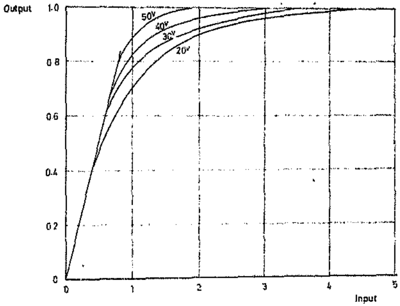

FIGURE 2.4

2.4 SCALING

The one aspect of the operation of an electronic analogue computer which perhaps causes more difficulty than any other is that of scaling. The need for scaling is obvious, for the computer variables are voltages, whereas there is a very wide range of problem variables, and it is essential to decide on suitable scale factors. In addition, many problems require scaling of the independent variable, which is usually time.

Paul[13], Levine[15] and Pfeffer[16] have discussed the factors to be considered when selecting amplitude scale factors. Voltages in the computer are limited by the operational amplifier design, varying from ± 100 volts for vacuum tube amplifiers to ± 10 volts for transistorised or integrated circuit amplifiers, and amplitude scale factors should be chosen so that this maximum voltage is not exceeded. Considerations of both amplifier noise and drift in integrators will determine the minimum voltage; once again this is determined by the amplifier design (see 2.21). Levine[15] has described a variable scaling technique when the range in problem variable is greater than the range in computer voltage. Levine has also made the following statement on the assessment of errors due to scaling : "A good empirical criterion for existing precision computers is that errors can result in a computer if the maximum voltage does not exceed one volt during the problem run".

The selection of suitable amplitude scale factors obviously requires prior knowledge of the likely range in the problem variables. While this could be obtained by trial and error, this would be very tedious on a large problem, and some other method is obviously desirable. Levine[15], quoting work by Jackson[18], describes the following method.

The differential equation describing the system is

$$\frac{d^n y}{dt^n} + a_{n-1}\frac{d^{n-1}y}{dt^{n-1}} + \text{———} + a_1 \frac{dy}{dt} + a_o y = B\ u(t) \qquad \text{where}$$

.../ the

the a's are constants. If B u(t) is a step forcing function of magnitude B, and if all initial conditions are zero, the maximum values of the variables can be approximated by

$$\left|\frac{d^n y}{dt^n}\right|_{max} = B$$

$$\left|\frac{d^r y}{dt^r}\right|_{max} = \frac{B}{a_r} \qquad 1 \leqslant r \leqslant n-1$$

$$\left| y \right|_{max} = \frac{2B}{a_o}$$

Levine[15] states that "there are no analytical methods that will indicate the maximum values of variables in large-scale non-linear, variable coefficient problems".

Pfeffer[16] has listed five factors to be taken into account in the determination of time scale factors :-

(i) integrator errors are increased by long computer runs;

(ii) long computer runs are usually associated with low and consequently inaccurate, potentiometer settings. In general, it is possible to tolerate runs of many minutes duration;

(iii) short computer runs are associated with high amplifier gains, and it is frequently necessary to cascade amplifiers to provide sufficient gain. This leads to cumulative phase shift, and imposes a maximum frequency of about 10 Hz, although in some cases errors are significant at lower frequencies;

(iv) the high frequencies associated with short runs cause phase shift in amplifiers, and thus lead to errors;

(v) it is necessary to consider the dynamics of the recording devices so that the response characteristics of the recorder do not affect the recording (see 2.1).

Harris[14], Levine[15] and Korn and Korn[17] have given useful rules for the application of both amplitude and time scaling factors.

3. THE POSITION CONTROL SERVOMECHANISM

3.1 GENERAL

Both West[5] and Hammond[8] have given general descriptions of the performance of a remote position control servomechanism when various non-linearities exist. This is a subject on which a fair number of papers has been written. As the main topic of this dissertation is the investigation of the performance of a remote position control servomechanism subject to torque limitation, this section contains a short summary of previous work.

West, Douce and Naylor[1] and West and Dalton[40] have considered the transient performance of a remote position control servomechanism possessing torque limitation. Both papers describe the use of the phase-plane to determine the step function response of the frictionless system when velocity feedback stabilisation is used. West and Dalton investigated the response to input steps up to one hundred times that just required to produce saturation, and concluded that the effect of saturation is to make the system more oscillatory. This effect, however, only becomes apparent at very large inputs, and the critically damped system first shows overshoot when the input step is twenty times that just necessary for saturation. West, Douce and Naylor investigated the use of error limitation as a method of stabilizing the non-linear system, and show how to select the value of error limitation which results in optimum response. In addition to the phase-plane analysis the authors carried out some experimental work on a servomechanism during which both velocity feedback and phase advance stabilization was used.

West and Nikiforuk[4,6] have used both the phase-plane method and an analogue computer to investigate the performance of a remote position control servomechanism with a 'hard-spring' non-linear characteristic. A 'hard-spring' non-linear

.../characteristic

characteristic is one in which the ratio of output to input increases with input. West[5] has justified the study of 'hard-spring' characteristics by pointing out that it is thought that muscle tensioning in animals follows a 'hard-spring' characteristic.

In their first paper the authors use an analogue computer to determine both frequency and transient response. The frequency response investigation was aimed at the location of points of discontinuity in the gain vs frequency and phase vs frequency plots. The transient response investigations revealed that the non-linearity improved the step function response without apparently affecting the stability of the system.

The second paper describes the use of the phase-plane method to investigate system performance when the non-linearity was approximated by a cubic equation. Velocity feedback stabilization was used, and the degree of damping was defined with reference to a similar linear system with a gain equal to the small signal gain of the non-linear system (see 3.2). Both the phase-plane method and an analogue computer were used to investigate system performance when the non-linearity was approximated by a segmented line. The use of phase-advance stabilization was also investigated.

Douce and King[12] describe the use of an analogue computer to obtain experimental results on the performance of a position control servomechanism. The system had a saturation-type non-linearity, and its response was obtained to repetitive step function inputs, a sinusoidal input signal and an input of Gaussian noise with a simple power spectrum. The servomechanism was fitted with a system whereby the damping factor was automatically adjusted to give a minimum mean squared error.

West and Somerville[41] considered the third-order system resulting when integral of error control is added to the normal second order frictionless position control servomechanism. The effects of torque limitation were investigated, and it was

.../found

found that instability arises when the system is subjected to large input steps. The phase-plane method was used to analyse the third order system, but could only be used for step input functions when initial velocities and accelerations were zero. The authors found that the addition of integrator output limiting was able to stabilise the system. Sections 3.2 and 3.3 are devoted to a study of a similar system, the only differences being the addition of viscous friction and motor field inductance.

Freeman[42] investigated the transient response of a position control servomechanism when backlash was present. The presence of backlash was found to make the system more oscillatory than the linear system.

Fallside and Ezeilo[43] and Fallside and Patel[44] have investigated the effect of a back e.m.f. non-linearity on the performance of a position control servomechamism. This non-linearity arises when the armature current supply has a non-infinite output impedance. Under these conditions the effect of armature back e.m.f. is to vary the armature current, and motor torque then becomes a non-linear function of field current and motor speed. The first paper applies an analytical technique to the analysis of the non-linear system, while in the second paper the phase-plane method is used to obtain the step function response of the system. The authors of this paper refer to the thesis of Fallside[45], which describes work on a similar system. In this work it was found that the effect of the back e.m.f. non-linearity depended upon the amount of viscous friction present. The non-linearity had little effect on system response when viscous friction was small, but the effect increased as the viscous friction was increased. This could be offset, however, by a reduction in the velocity feedback, so that the total damping remained constant. This is the approach adopted in the following section, where the amount of velocity feedback depends on the viscous friction, the total damping remaining constant.

.../3.2

3.2 THEORETICAL ANALYSIS OF LINEAR OPERATION

3.21 General Theory

The basic equations describing the linear operation of a position control servomechanism utilising velocity feedback and integral of error control are given below. The servomechanism is assumed to use a split field d.c. motor, control being obtained through control of the field current. Douce[39] has considered the effect of field current inductance and it can be seen that the effect of this has been included here. The effects of viscous friction have also been included.

$$e = K_1 \left(1 + \frac{1}{sT_1}\right) (\theta_i - \theta_o) - sK_4\theta_o$$

$$L = \frac{K_2}{1 + sT_2} \quad e = s^2 m\theta_o + sK_3\theta_o$$

No account has been taken of the back e.m.f. non-linearity dealt with by Fallside and Ezeilo[43], Fallside and Patel[44], and Fallside[45].

These equations lead to the differential equation governing the operation of the servomechanism when the feedback loop is closed.

$$s^2 (1 + sT_2)\,\theta_o + s\,\frac{1}{m}\left\{K_3 (1 + sT_2) + K_2K_4\right\}\theta_o$$

$$+ \frac{K_1K_2}{m} \left(1 + \frac{1}{sT_1}\right)\theta_o = \frac{K_1K_2}{m} \left(1 + \frac{1}{sT_1}\right)\theta_i \text{ —— } (2)$$

When $T_1 \longrightarrow \infty$ and $T_2 = 0$ it can be seen that this equation reduces to the familiar second order system equation

.../ s^2

$$s^2 \theta_o + s \frac{1}{m} (K_3' + K_2K_4) \theta_o + \frac{K_1K_2}{m} \theta_o = \frac{K_1K_2}{m} \theta_i$$

If this is compared with the 'standard' form of the second order equation, i.e.

$$s^2\theta_o + 2 \lambda w_n s\theta_o + w_n^2\theta_o = w_n^2\theta_i$$

it can be seen that for the second order system

$$w_n = \sqrt{\frac{K_1K_2}{m}}$$

and

$$\lambda = \frac{K_3 + K_2K_4}{2 \sqrt{K_1K_2m}}$$

The open loop transfer function for the system is

$$\frac{\theta_o}{\theta_i} = \frac{\frac{-K_1K_2}{m} (s + \frac{1}{T_1})}{s^2 \left\{ s^2T_2 + (1 + \frac{K_3T_2}{m}) s + \frac{1}{m} (K_3 + K_2K_4) \right\}}$$

This equation can be re-written in terms of w_n and λ as defined above, and the two dimensionless variables α and x.

$$\frac{\theta_o}{\theta_i} = \frac{- w_n^2 (s + \frac{1}{T_1})}{s^2T_2 (s^2 + \frac{1}{T_2} (1 + \alpha x) s + \frac{\alpha}{T_2^2})}$$

$$\alpha = 2 \lambda w_n T_2$$

$$= \frac{T_2}{m} (K_3 + K_2K_4)$$

$$x = \frac{K_3}{K_3 + K_2K_4} = \frac{K_3}{2 \lambda w_n m}$$

.../ The

The use of the above definitions for w_n and λ can be compared with the method used by West and Nikiforuk[6] in defining the damping constant in a non-linear system in terms of the damping constant in the small signal linear system.

The open loop transfer function can also be written

$$\frac{\theta_o}{\theta_i} = \frac{-w_n^{\,2}\left(s+\frac{1}{T_1}\right)}{s^2T_2\left\{s+\frac{1}{2T_2}(1+\alpha x+y)\right\}\left\{s+\frac{1}{2T_2}(1+\alpha x-y)\right\}}$$

where $\quad y = \sqrt{(1+\alpha x)^2 - 4\alpha}$

Thus it is the values of both α and x which determine the nature of the open loop poles. The open loop transfer function will have real poles when $(1+\alpha x)^2 > 4\alpha$, and two complex poles when $(1+\alpha x)^2 < 4\alpha$. A real pole of second order exists when $(1+\alpha x)^2 = 4\alpha$. Figure 3.1 is a plot of the function $4\alpha = (1+\alpha x)^2$, and thus shows the division of the α, x plane into complex and real pole regions. (The points marked on this figure show the α, x combinations for which the servomechanism response was calculated).

The root locus method is commonly used (see e.g. Truxal[10] or Thaler and Brown[46]) for locating the poles of the closed loop transfer function once the positions of the poles and zeros of the open loop transfer function are known. The root loci consist of all points in the s plane at which the phase of the open loop transfer function is $0^\circ + n360^\circ$, where n has any integral value. As normally used, it is the value of the gain of the system which determines at which points on the loci the closed loop poles are situated, and it is assumed that the gain is an independent variable which can be changed so as to obtain a suitable closed loop pole configuration. Inspection of the equation for the open loop transfer function of the position control servomechanism shows that the 'gain' $\frac{w_n^{\,2}}{T_2}$ is in this case not an independent variable,

.../as

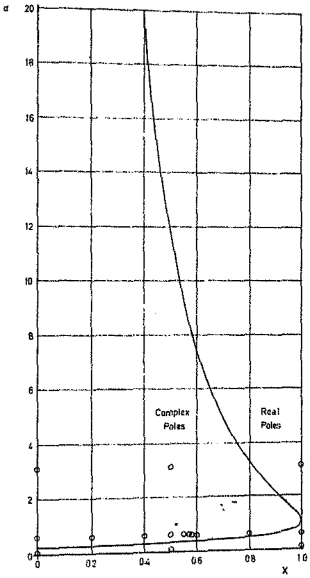
α
20
18
16
14
12
10
8
6
4
2
0
0
0.2
0.4
0.6
0.8
1.0
X
Complex Poles
Real Poles

FIGURE 3.1

as the positions of the open loop poles are determined by the values of both w_n and T_2. This does not mean that the root locus method cannot be applied to the problem, what it does mean is that, except in circumstances to be covered below, the root loci have no physical significance except at points where the gain is $\frac{w_n^2}{T_2}$, in other words they are no longer, strictly speaking, loci.

3.22 Normalisation

In the equations so far developed both α and x are dimensionless quantities, and in view of the very much increased usefulness of general solutions it seemed worthwhile to investigate the possibility of using some form of time normalisation in the analysis of the servomechanism operation.

Following the description of time normalisation given by Tustin[47], the closed loop transfer function is first obtained

$$\frac{\theta_o}{\theta_i} = \frac{1 + s\,T_1}{1 + sT_1 + s^2\, 2\lambda \frac{T_1}{w_n} + s^3 \frac{T_1}{w_n^2}(1 + \alpha x) + s^4 \frac{T_1 T_2}{w_n^2}}$$

if $s_o = s \sqrt[4]{\frac{T_1 T_2}{w_n^2}}$ this expression becomes

$$\frac{\theta_o}{\theta_i} = \frac{1 + s_o \sqrt[4]{\frac{T_1^3\, w_n^2}{T_2}}}{1 + s_o \sqrt[4]{\frac{T_1^3 w_n^2}{T_2}} + s_o^2\, 2\lambda\sqrt{\frac{T_1}{T_2}} + s_o^3 \sqrt[4]{\frac{T_1}{w_n^2 T_2^3}}(1 + \alpha x) + s_o^4}$$

.../This

This indicates that system responses can be obtained as a function of dimensionless time $\sqrt[4]{\frac{w_n^2}{T_1 T_2}}\, t$, three dimensionless parameters,

$\sqrt[4]{\frac{T_1^3\, w_n^2}{T_2}}$, $2\sqrt{\frac{T_1}{T_2}}$ and $\sqrt[4]{\frac{T_1}{w_n^2 T_2^3}}\;(1 + \alpha x)$ being required to specify the system constants.

If the three dimensionless parameters are denoted A_1, A_2 and A_3 –

$$A_1 = \sqrt[4]{\frac{T_1^3\, w_n^2}{T_2}}$$

$$A_2 = 2\lambda\sqrt{\frac{T_1}{T_2}}$$

$$A_3 = \sqrt[4]{\frac{T_1}{w_n^2 T_2^3}}\;(1 + \alpha x)$$

the closed loop transfer function becomes

$$\frac{\theta_o}{\theta_i} = \frac{1 + s_o A_1}{1 + s_o A_1 + s_o^2 A_2 + s_o^3 A_3 + s_o^4}$$

while the open loop transfer function is

$$\frac{\theta_o}{\theta_i} = \frac{-(1 + s_o A_1)}{s_o^2\,(s_o^2 + s_o A_3 + A_2)}$$

…/ –

$$= \frac{-(1 + s_o A_1)}{s_o^{\,2}\left\{s_o + \tfrac{1}{2} A_3 + j\sqrt{A_2 - \tfrac{1}{4} A_3^{\,2}}\right\}\left\{s_o + \tfrac{1}{2} A_3 - j\sqrt{A_2 - \tfrac{1}{4} A_3^{\,2}}\right\}}$$

While analysis of the system using the normalised open and closed loop transfer functions derived above must lead to a better understanding of its operation, and of the interaction of the various parameters, it is not necessarily the most convenient method of approach. Thus, an investigation into the effects of the value of the integrator time constant (T_1), by means of the root locus method, will only involve the calculation of one set of open loop pole positions should the original equations be used. Use of the normalised equations will involve the calculations of a complete set of open loop pole and zero positions for each value of T_1.

It is worthwhile investigating the situation when time is 'normalised' in terms of the natural frequency w_n.

On the assumption that the closed loop transfer function has been obtained for the case when $T_2 = T$ and $w_n = W$, and the integrator has a time constant T_1, a general solution is required when $w_n T_2 = WT$ and α and x are unchanged. The integrator in this case has a time constant of T_1'.

If $T_2 = BT$ the requirement that $w_n T_2 = WT$ leads to $w_n = \frac{W}{B}$, and if in addition $T_1' = BT_1$ the following expressions for the open loop transfer functions can be obtained.

(i) $w_n = W, T_2 = T,$

$$\frac{\theta_o}{\theta_i} = \frac{-W^2\left(s + \frac{1}{T_1}\right)}{s^2 T\left\{s + \frac{1}{2T}(1 + \alpha x + y)\right\}\left\{s + \frac{1}{2T}(1 + \alpha x - y)\right\}}$$

.../ (ii)

(ii) $w_n = \frac{W}{B}$, $T_2 = BT$,

$$\frac{\theta_o}{\theta_i} = \frac{-W^2\ (s + \frac{1}{BT_1})}{s^2B^3T\left\{s + \frac{1}{2BT}\ (1 + \alpha x + y)\right\}\left\{s + \frac{1}{2BT}\ (1 + \alpha x - y)\right\}}$$

if S = Bs this becomes

$$\frac{\theta_o}{\theta_i} = \frac{-W^2\ (S + \frac{1}{T_1})}{BS^2T\left\{S + \frac{1}{2T}\ (1 + \alpha x + y)\right\}\left\{S + \frac{1}{2T}\ (1 + \alpha x - y)\right\}}$$

These equations show that closed loop characteristics cannot be obtained in terms of these 'normalised' values, but on the other hand, all systems with constant values of x, α , w_nT_1, and w_nT_2 have identical open loop poles and zeros, and hence their closed loop poles lie on the same root 'loci'. The gain term now becomes $\frac{W^2}{BT}$.

3.23 Step Function Responses of Selected Systems

In further investigating the operation of the position control servomechanism, the following numerical values were chosen -

w_n = 3,16 s^{-1} $\therefore$ w_n^2 = 10 s^{-2}

λ = 1,0

The following combinations of x, T_1 and T_2 were used -

(i) With x = 0,5, T_2 = 0,02, 0,1, 0,5 s (α = 0,1265, 0,633, 3,16)

.../ T_1

T_1 was varied from 0,1 s to ∞ ($\frac{1}{T_1}$ from 0 to 10 s^{-1})

(ii) With $T_1 \longrightarrow \infty (\frac{1}{T_1} = 0)$ x = 0, 1,0 and T_2 = 0,02, 0,5 s (α = 0,1265, 3,16)

(iii) With $T_1 \longrightarrow \infty (\frac{1}{T_1} = 0)$, T_2 = 0,1 s (α = 0,633) x was varied from 0 to 1,0.

Figures 3.2, 3.3 and 3.4 show the 'root locus' plots for the combinations mentioned in (i) above, The points on the loci where the gain = $\frac{w_n^2}{T_2}$ are shown; these are the positions of the closed loop poles.

Figures 3.5, 3.6 and 3.7 show only the open loop pole positions and closed loop pole loci for the above figures. In all cases the effect of integrator time constant T_1 upon the stability of the system is evident, low values of T_1 leading to poles with positive real parts and hence to an unstable system.

Figure 3.8 shows the variation of open and closed loop poles for condition (iii) above, where x is varied from 0 to 1. The open loop poles (for $0 < x < 0{,}934$) can be seen to lie on a circle centred at the origin, and this follows from the fact that open loop poles exist where

$$s = -\frac{1}{2T_2}\left(1 + \alpha x \pm j\sqrt{4\alpha - (1 + \alpha x)^2}\right)$$

Since $s = \sigma + jw$

It follows that $\sigma = \frac{1}{2T_2}(1 + \alpha x)$

and $w = -\frac{1}{2T_2}\left(\pm\sqrt{4\alpha - (1 + \alpha x)^2}\right)$

.../whence

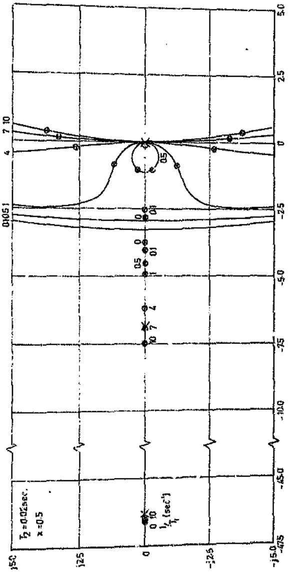

FIGURE 3.2

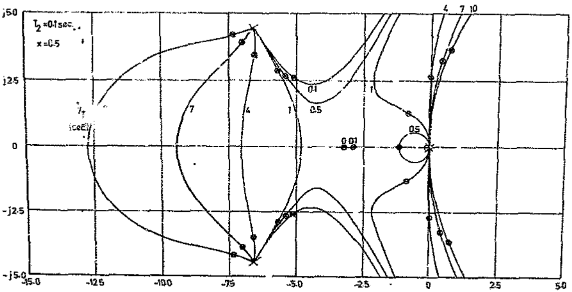

T_2 = 0.1 sec.
x = 0.5
j5.0
j2.5
0
-j2.5
-j5.0
-15.0
-12.5
-10.0
-7.5
-5.0
-2.5
0
2.5
5.0
4
7
10
0.1
0.5
1
7
4
1
0.5
0 0.1
0.5
T_1 (sec)

FIGURE 3.3

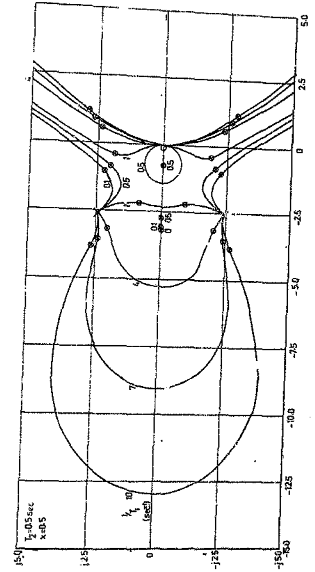

T_z=0.5 sec
x=0.5
$1/\tau_t$ (sec)
j5.0
j2.5
0
-j2.5
-j5.0
5.0
2.5
0
-2.5
-5.0
-7.5
-10.0
-12.5
-15.0

FIGURE 34

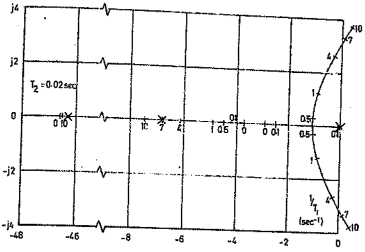

FIGURE 3·5

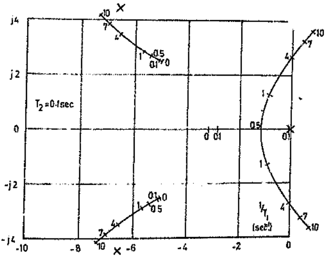

FIGURE 3·6

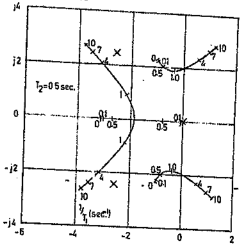

FIGURE 3.7

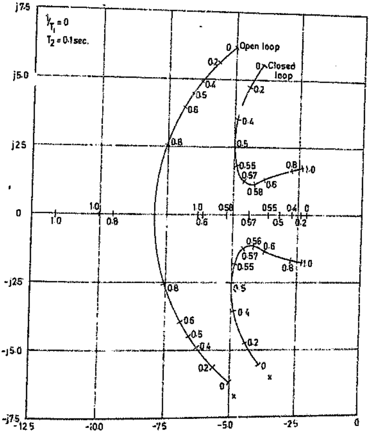

FIGURE 3.8

whence $\sigma^2 + w^2 = \left(\sqrt{\frac{\alpha}{T_2}}\right)^2$

Thus, for constant α, open loop poles are situated on a circle centred at the origin with radius $\sqrt{\frac{\alpha}{T_2}}$

Knowledge of the closed loop pole positions leads to the closed loop transfer function in rational algebraic form. The evaluation of system responses to given input functions is then achieved by the use of Laplace - transform theory. (See for example Truxal[10] or Bronwell[48]). In this instance the step function responses of the various systems were calculated. Figures 3.9 to 3.14 show the results obtained, and once again the marked effect of integrator time constant on system stability is apparent.

The step function response of the system described in (iii) above (figure 3.13) is worthy of mention. Examination of figure 3.8 shows that the closed loop pole configurations for the three cases x = 0, x = 0,5, x = 1,0 differ considerably, with surprisingly little effect upon the step function response.

3.3 ANALOGUE COMPUTER ANALYSIS OF BOTH LINEAR AND NON-LINEAR OPERATION

The operation of the position control servomechanism in the non-linear region was investigated by using an analogue computer. It was assumed that the torque of the system was limited, and the analogue computer was used to determine step function responses in the linear region, and in the non-linear region where the servomechanism was subjected to torque limitation and to torque limitation together with limitation of the integrator output.

The most common method of simulating saturation type non-linearities on an analogue computer is by the use of diodes. Appendix 6.1 gives details of measurements of non-linearity in an

.../actual

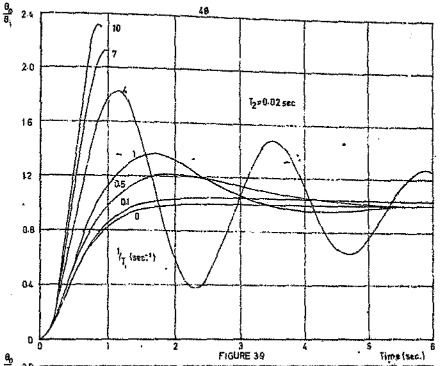

FIGURE 3.9

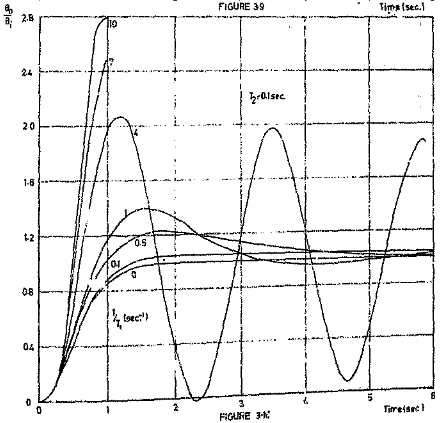

FIGURE 3.10

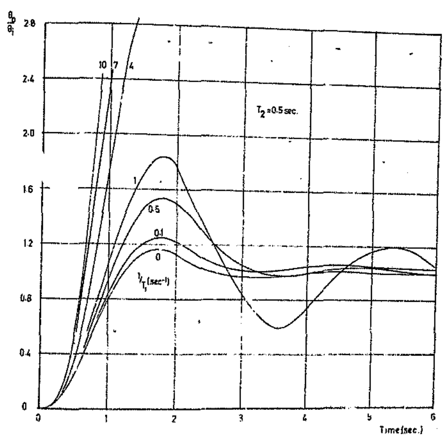

$\frac{\theta_o}{\theta_i}$
2.8
2.4
2.0
1.6
1.2
0.8
0.4
0
10
7
4
1
0.5
0.1
0
$\frac{1}{T_1}$ (sec^{-1})
T_2 = 0.5 sec.
0
1
2
3
4
5
6
Time (sec.)

FIGURE 3·11

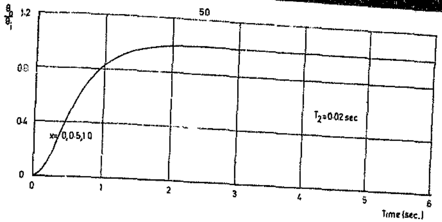

FIGURE 3-12

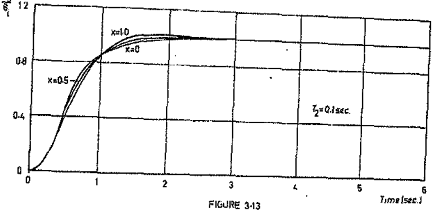

FIGURE 3-13

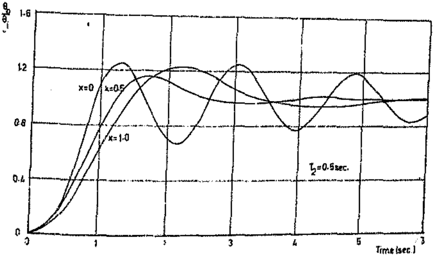

FIGURE 3-14

actual amplifier-split field d.c. motor system while 2.31 gives the results of tests on an analogue circuit using diodes. It can be seen that diodes can provide a good approximation to actual saturation curves.

In simulating the operation of the position control servomechanism it was convenient to use three different circuit layouts on the analogue computer. These three circuits all had identical characteristics in the linear region, the differences arising in the arrangements for simulating the saturation non-linearities. Figures 3.15, 3.16 and 3.17 show the three circuit layouts used, and also give the transfer functions of the individual operational amplifiers.

In all cases the differential equation describing operation in the linear region was -

$$s^2 (1 + 0{,}0198\ s)\ \theta_o + s\,\frac{1}{m}\left(K_3 (1 + 0{,}0198\ s) + K_2K_4\right) \theta_o$$

$$+ 10\left(1 + \frac{1}{sT_1}\right) \theta_o = 10\left(1 + \frac{1}{sT_1}\right) \theta_i$$

Comparison with equation 2 shows that $w_n = 3.16\ s^{-1}$ and $T_2 = 0{,}0198$ s. The constants $\frac{K_3}{m}$ and $\frac{K_2K_4}{m}$ could be varied independently, but these variations were in most cases such that

$$\frac{K_3}{m} + \frac{K_2K_4}{m} = 2\sqrt{10} \quad \text{and therefore } \lambda = 1{,}0$$

$$\text{and} \qquad \alpha = 0{,}125$$

Initial tests were done to determine the step function response of the linear system for different values of the damping factor λ and the integrator time constant T_1. The results of these tests are summarised in figures 3.18, 3.19 and 3.20, where the rise time, overshoot and settling time of the system are

.../plotted

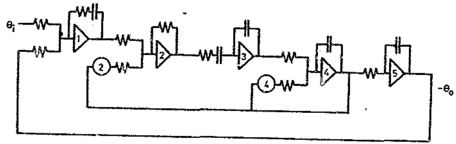

Operational Amplifier	Transfer Function	
1	$-0.422(1+(sT)^{-1})(v_1+v_2)$	$0.1<T<1.05$ sec, $T\to\infty$
2	$-(1.0v_1+10r_2v_2)$	$0<r_2<1.0$
3	$-0.982(1+sT)^{-1}$	$T=0.0198$ sec
4	$-(1.0v_1+10r_4v_2)(sT)^{-1}$	$T=0.203$ sec, $0<r_4<1.0$
5	$-(sT)^{-1}$	$T=0.204$ sec

(n) Operational amplifier

(n) · Potentiometer

v_n Input(s) to operational amplifier

r_n Potentiometer setting

FIGURE 3.15

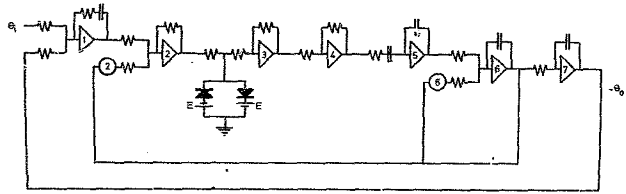

Operational Amplifier	Transfer Function	
1	$-0.422(1+(sT)^{-1})(v_1+v_2)$	$T = 1.05$ sec
2	$-(1.0v_1+20r_2v_2)$	$0<r_2<1.0$
3	$-0.5v_1$ $\lvert output \rvert = E$	$\lvert v_1 \rvert < 2E$ $\lvert v_1 \rvert > 2E$
4	-0.2	
5	$-0.982(1+sT)^{-1}$	$T = 0.0198$ sec
6	$-(1.0v_1+10r_6v_2)(sT)^{-1}$	$T = 0.203$ sec, $0<r_6<1.0$
7	$-(sT)^{-1}$	$T = 0.204$ sec

FIGURE 3-16

n Operational amplifier

(n) Potentiometer

v_n Input(s) to operational amplifier

r_n Potentiometer setting

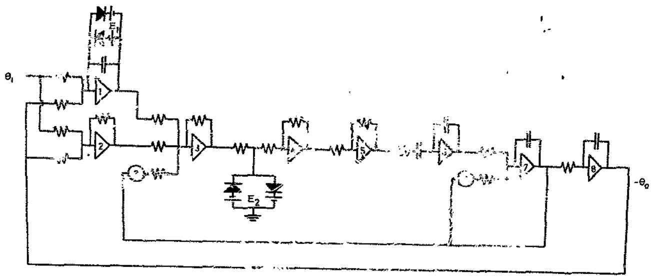

Operational Amplifier	Transfer Function	
1	$-0.422(sT)^{-1}(v_1+v_2)$	$T=1.05$ sec, $\lvert output \rvert < E_1$
	$\lvert output \rvert = E_1$	
2	$-0.422(v_1+v_2)$	
3	$-(1.0v_1+1.0v_2+2.0r_3v_3)$	$0<r_3<1.0$
4	$-0.5v_1$	$\lvert v_1 \rvert < 2E_2$
	$\lvert output \rvert = E_2$	$\lvert v_1 \rvert > 2E_2$
5	-0.2	
6	$-0.982(1+sT)^{-1}$	$T=0.0198$ sec
7	$-(1.0v_1+1.0r_7v_2)(sT)^{-1}$	$T=0.203$ sec, $0<r_7<1.0$
8	$-(sT)^{-1}$	$T=0.204$ sec

FIGURE 3-17

(n) Operational amplifier

(r) Potentiometer

v_n Input(s) to operational amplifier

r_n Potentiometer setting

plotted against T_1^{-1} for various values of λ .

All subsequent work was carried out with $\lambda = 1,0$, $T_1 = 1,05$ sec. Figure 3.21 shows the step function response of the linear system for various values of T_1, the integrator time constant. These results can be compared with figure 3.9 which shows the calculated results for the same system. In general the results can be seen to agree fairly well, with the exception of the curve for $T_1 \longrightarrow \infty (\frac{1}{T_1} = 0)$. Here, the analogue results indicate a fairly slow response, about 5 s being required for the output to reach within 1% of the input. The corresponding time for the calculated results is about 2 s. A possible reason for this discrepancy is the difficulty experienced in reading accurately the analogue records, for the full deflection due to the step input was only about 20 mm.

The step function responses for the non-linear systems are shown in figures 3.22 - 3.27. These all show the servomechanism response to an input step which is 10 times the size of the step just necessary to cause the torque to reach its saturation level. The saturation level of the integrator output is defined in terms of the torque saturation level. A saturation level ratio of unity occurs when the saturated output of the integrator is sufficient to cause the torque to become saturated, in the absence of other signals.

The curves for an infinite saturation level ratio given in figures 3.22 - 3.27 show that the effect of viscous friction is to stabilise the system. (An infinite saturation level ratio corresponds to torque limitation only). The stabilisation, however, is not accompanied by a marked improvement in system response, which becomes oscillatory with very little damping. Figure 3.28 is a phase-plane plot of the step function response of the system with infinite saturation level ratio. This plot emphasises the periods of constant velocity operation of those systems with large amounts of viscous friction.

Figures 3.22 - 3.27 also show the step function responses of systems with finite values of the saturation level ratio. The

.../stabilisation

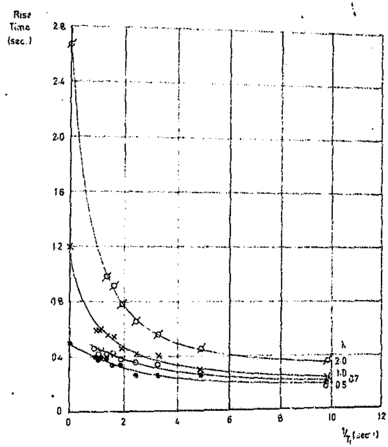

FIGURE 3.18

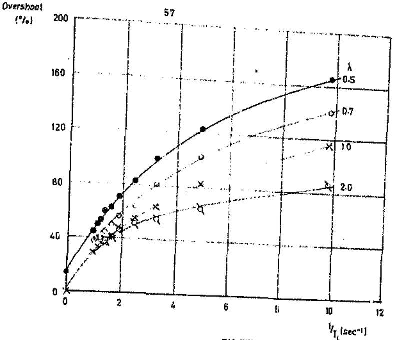

FIGURE 3-19

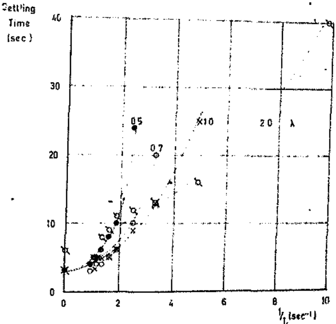

FIGURE 3-20

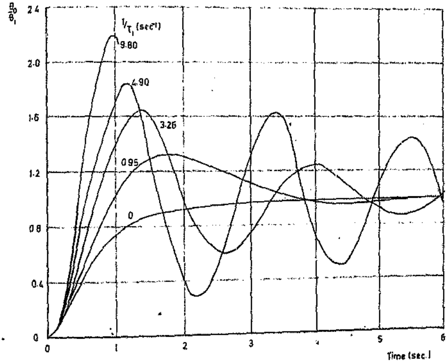

$\frac{\theta_0}{\theta_i}$
2.4
2.0
1.6
1.2
0.8
0.4
0
$1/T_1$ (sec^{-1})
9.80
4.90
3.26
0.95
0
0
1
2
3
4
5
6
Time (sec.)

FIGURE 3·21

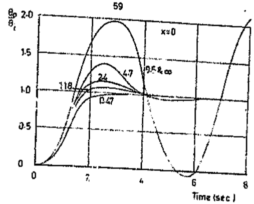

FIGURE 3-22

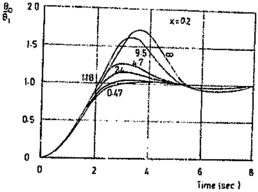

FIGURE 3-23

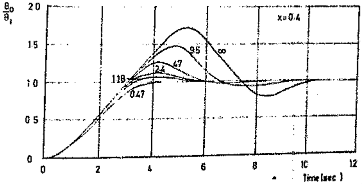

FIGURE 3-24

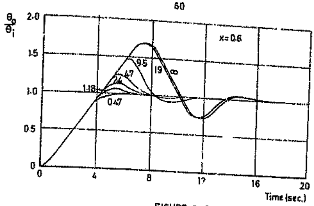

FIGURE 3·25

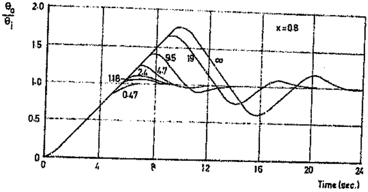

FIGURE 3·26

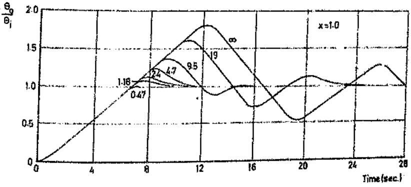

FIGURE 3·27

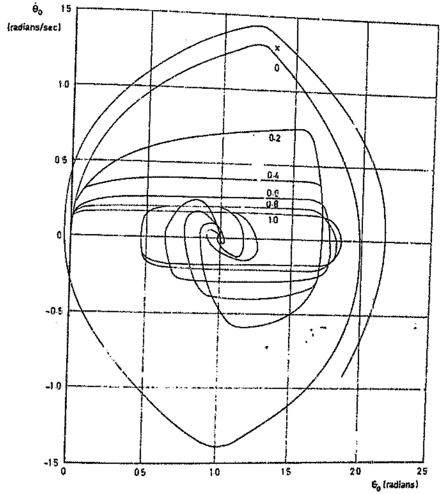
$\dot{\theta}_0$ (radians/sec)
1.5
1.0
0.5
0
-0.5
-1.0
-1.5
0
0.5
1.0
1.5
2.0
2.5
θ_0 (radians)
x
0
0.2
0.4
0.6
0.8
1.0

FIGURE 3-28

stabilisation and improvement in system response brought about by the introduction of integrator limiting is apparent. The preliminary selection of an optimum value for the saturation level ratio can be made from an examination of the step function responses shown in figures 3.22 - 3.27, and it would seem that ratios between 0.47 and 1.18 would provide the optimum response to a step function input ten times that necessary to cause torque saturation.

Figures 3.29 - 3.34 show the response of a system with equal saturation levels (unity saturation level ratio) to different sizes of input step. These figures show that the system response, if judged on the basis of time to equilibrium, or settling time, is, for any particular value of x (the proportion of the damping due to viscous friction), substantially independent of the size of the input step. As would be expected the settling time depends to a very large extent upon the amount of viscous friction.

Figures 3.35 - 3.38 are further plots of the response of the system with equal saturation levels when subjected to an input step ten times the size necessary to cause torque saturation. Figure 3.35 is a conventional output against time plot. The effect of variations in x is very marked. Figure 3.36 is a phase-plane plot, while figure 3.37 shows the variation in output velocity with time. Both of these figures show that torque limitation becomes in effect velocity limitation once the amount of viscous friction becomes appreciable. Figure 3.38 is a plot of torque against time. The graph for x = 0 shows that the system twice entered the region of torque saturation, and it is evident that the positive and negative torque saturation levels were not identical, and in fact differed by about 10%.

This section will be concluded with a few general comments on the operation of the analogue computer.

The determination of the response of a non-linear system to various inputs can be made very easily on the analogue computer. The accuracy should be adequate for most practical problems. Experience on this work has confirmed the comments made by Pfeffer[16]

.../(section

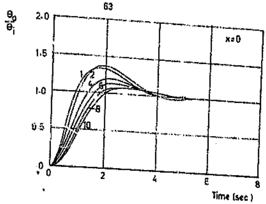

FIGURE 3·29

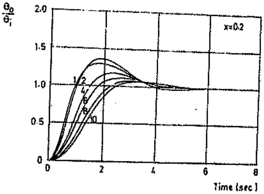

FIGURE 3·30

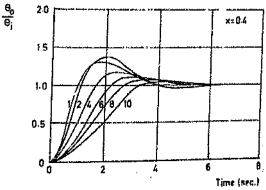

FIGURE 3·31

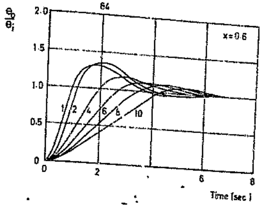

FIGURE 3.32

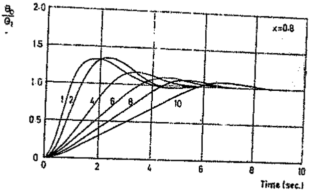

FIGURE 3.33

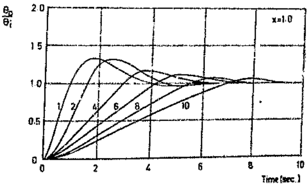

FIGURE 3.34

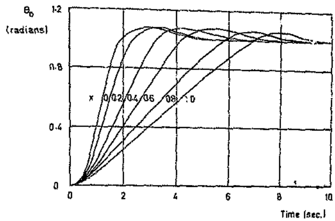

FIGURE 3·35

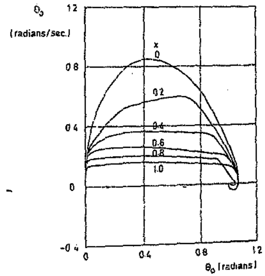

FIGURE 3·36

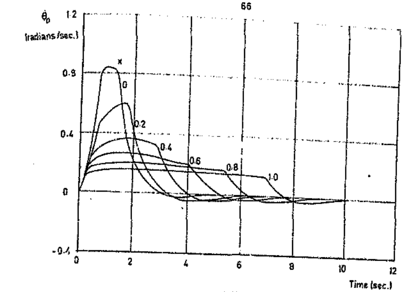

FIGURE 3·37

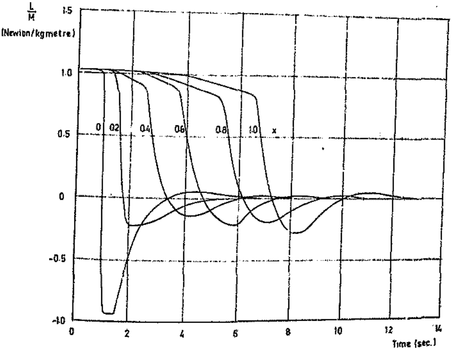

FIGURE 3·38

(section 2.1). The recorder used was probably the major source of error in the solution, and in addition a great deal of time and effort was spent in reading and examining the very small records. The use of a potentiometer type recorder, or a servo x - y plotter, would have resulted in large improvements in accuracy and would, in addition, have made the reading of records very much easier.

The disadvantage of using an analogue computer lies in the fact that it does not generally lead to a proper insight into the whole problem, such as is generally obtained from an analysis of a linear system or from an analysis (such as the phase-plane) of a non-linear system. The analogue computer can only solve those problems put to it, and it remains for the operator to seek to get a general understanding of the system.

4. REFERENCES

(1) West, J.C., Douce, J.L., and Naylor, R. : "The Effects of the addition of some non-linear elements on the transient performance of a simple R.P.C. system possessing torque limitation". Proceedings I.E.E., Paper No. 1549 M August, 1953 (101, Part II, p. 156).

(2) Holt-Smith, C. : Contribution to above paper.

(3) Coales, J.F. : Contribution to above paper.

(4) West, J.C. and Nikiforuk, P.N. : "The Behaviour of a remote-position-control servomechanism with hard spring non-linear characteristics". Proceedings I.E.E., Paper No. 1621 March, 1954 (101, Part II, p. 481).

(5) West, J.C. : "Analytical Techniques for non-linear control systems". The English Universities Press. 1960.

(6) West, J.C. and Nikiforuk, P.N. : "The response of remote-position-control systems with hard-spring non-linear characteristics to step function and random inputs". Proceedings I.E.E., Paper No. 1728 M, October, 1954 (102, Part B, p. 575).

(7) Tustin, A. : Contribution to above paper.

(8) Hammond, P.H. : "Feedback theory and its applications". English Universities Press, 1958.

(9) Thaler, G.J. and Pastel, M.P. : "Analysis and design of non-linear feedback control systems". McGraw-Hill, 1962.

(10) Truxal, J.G. : "Automatic feedback control system synthesis". McGraw-Hill, 1955.

.../ (11)

(11) Kalman, R.E. : "Analysis and design principles of second and higher order saturating servomechanisms". Transactions A.I.E.E. 1955,(74 Part II, p. 294).

(12) Douce, J.L., and King, R.E. : "A self-optimising non-linear control system". Proceedings I.E.E., Paper No. 3523 M, July, 1961, (108, Part B, p. 441).

(13) Paul, R.J.A. : "Fundamental analogue techniques". Blackie and Son, 1965.

(14) Harris, D.J. : "Analogue and digital computer methods". Temple Press, 1964.

(15) Levine, L. : "Methods for solving engineering problems using analog computers". McGraw-Hill, 1964.

(16) Pfeffer, I. : "Linear electronic computer elements". Chapter 22 of "Handbook of automation, computation and control, Vol. 2" edited by E.M. Grabbe, S. Ramo, and D.E. Wooldridge, John Wiley, 1959.

(17) Korn, G.A. and Korn, T.M. : "Electronic analog computers" 2nd ed. McGraw-Hill, 1956.

(18) Jackson, A.S. : "Analog computation". McGraw-Hill, 1960.

(19) Pearlman, A. : "Selecting and testing solid-state operational amplifiers". Instruments and Control Systems, Feb. 1965, p. 121.

(20) Markkula, A.O. : "Practical considerations in the design of systems using linear integrated circuits". Chapter 20 of "Application considerations for linear integrated circuits" edited by J. Eimbinder Wiley-Interscience, 1970.

..." (21)

(21) Stata, R. : "Interpreting operational amplifier specifications" Chapter 2 of book quoted in (20) above.

(22) Routh, W. : "Applications for operational amplifiers". Chapter 3 of book quoted in (20) above.

(23) "Applications manual for computing amplifiers". Philbrick Researches Inc. 1966.

(24) Curtis, A.J. : "Dielectric properties of polymeric systems" from "Progress in dielectrics Volume 2", edited by J.B. Birks, Heyw..., 1960.

(25) Broens, O. and Müller, F.H. : Kolloid Z. 140, 121 (1955); 141, 20 (1955).

(26) Von Hippel, A. : "Dielectric materials and applications". Chapman and Hall, 1954.

(27) Birks, J.B. : "Modern dielectric materials". Temple Press

(28) Charlton, C.B. and Shen, T.E. : "Plastic film - dielectric capacitors" Proceedings I.E.E. Paper No. 3697, February, 1962, (109 B, Supplement No. 22, p. 476).

(29) Dummer, G.W.A. : "Modern electronic components". Pitman, 1966.

(30) Hartshorn, L., Parry, J.V.L. and Rushton, E. : "The diele...ic losses in some representative insulating materials". Proceedings I.E.E., Paper No. 1451, February, 1953, (100, Part II A, p. 23).

(31) Dummer, G.W.A. : "Fixed Capacitors". Pitman, 1964.

(32) Dummer, G.W.A. : "Fixed resistors". Pitman, 1956.

(33) Church, H.F. : "The long-term stability of fixed resistors". Proceedings I.E.E. Paper No. 3277 E, July 1960 (107, Part B, p. 377).

(34) Church, H.F. : Reply to discussion on above paper. Proceedings I.E.E. (109, Part B, Supplement No. 21).

(35) Braner, H., and Easterday, J.L. : "Life characteristics of carbon-film resistors after 12,000 hours of operation". Transactions A.I.E.E. 1959,(78 Part I, p. 201).

(36) Osborne, S. : "The high frequency performance of helical film resistors". Proceedings I.E.E., Conference on components and materials used in electronic engineering. Conference publication No. 12, 1965.

(37) Millard, G.H. : "Measurements of non-linearity in cracked carbon resistors". Proceedings I.E.E., Paper No. 2747 R, January, 1959 (106, Part B, p. 31).

(38) Kirby, P.L. : "Third harmonic index as a measure of the non-linearity of fixed resistors". Proceedings I.E.E., Conference on components and materials used in electronic engineering. Conference publication No. 12, 1965.

(39) Douce, J.L. : "An introduction to the mathematics of servo-mechanisms". English Universities Press, 1963.

(40) West, J.C. and Dalton, I.R. : "The step function response of an R.P.C. servomechanism possessing torque limitation". Proceedings I.E.E., Paper No. 1576, November, 1953 (101, Part II, p. 166).

.../ (41)

(41) West, J.C. and Somerville, M.J. : "Integral control with torque limitation". Proceedings I.E.E., Monograph No. 181 M, June, 1956 (103, Part C, p. 407).

(42) Freeman, E.A. : "An approximate transient analysis of a second-order position-control system when backlash is present". Proceedings I.E.E., Monograph No. 254 M September, 1957 (105, Part C, p. 61).

(43) Fallside, F. and Ezeilo, J.O.C. : "Application of the second method of Lyapunov to the stability of certain position control systems containing a back - e.m.f. non-linearity". Proceedings I.E.E. paper No. 4273 S, December, 1962 (110, p. 1855).

(44) Fallside F. and Patel, M.R. : "Effect of a back e.m.f. non-linearity on responses of a second-order position control system". Proceedings I.E.E. Paper No. 4312 S, June, 1963, (110, p. 1867).

(45) Fallside, F. : "Non-linear servomechanism transient response". Ph. D. Thesis, University of Wales, 1958.

(46) Thaler, G.J. and Brown, R.G. : "Servomechanism analysis". McGraw-Hill, 1953.

(47) Tustin, A. : "Similarity and dimensional relationships in control systems". Proceedings I.E.E. Paper No. 2652 M, November, 1958 (105, Part C, Supplement No. 1, p. 58).

(48) Bronwell, A. : "Advanced Mathematics in Physics and Engineering". McGraw-Hill, 1953.

5. LIST OF SYMBOLS

This list of symbols is not complete, for there are some symbols which are adequately described in the text and have not been included. There is also some duplication of symbols. Where this has occurred the context should generally eliminate confusion.

α	resistor temperature coefficient, system constant
δ	capacitor loss angle
λ	damping factor
ϕ	motor flux per pole
θ	angular position
a	number of pairs of parallel armature circuits
e	error voltage, voltage
j	$\sqrt{-1}$
m	system moment of inertia
p	number of pole pairs
s	complex Laplace operator ($= \sigma + jw$)
w	angular frequency
w_n	natural frequency
x	proportion of damping due to viscous friction
y	constant
A	amplifier gain ($A = f(w)$), constant
B	resistor dissipation constant, constant
C	capacitance
E	voltage
K	constant
L	motor torque, inductance
M	mutual inductance
P	resistor power dissipation
Q	resistance
R	resistance

.../ S

S	resistance
T	time constant, temperature
T_1	integrator time constant
T_2	motor field circuit time constant
Z	impedance
Z_a	total number of armature conductors, amplifier input impedance
Z_L	amplifier load impedance

Subscripts

f	feedback
i	input
o	output

6. APPENDICES

6.1 Measurement of Saturation in Servomechanism Components

Tests were carried out on a d.c. power amplifier and split field d.c. motor to determine the shape of the saturation curve. Table 6.1 shows the results of tests on the amplifier, while tables 6.2 and 6.3 give the results of the motor tests. It can be seen that the motor was tested at no load (table 6.2), the armature current, with the exception of the first two tests, being about 0,1 amp, and at zero speed (table 6.3), the armature current in this case being 0,78 amps. The results of both tests were used to calculate the product $\frac{2p}{2a} Z_a \phi$.

Input voltage volts	Output current mA		
	Field 1	Field 2	Nett
0	32	32	0
0,02	27	36	9
0,04	23	40	17
0,06	20	42	22
0,08	17	45	28
0,10	13	4[illegible]	35
0,15	7	53	46
0,20	2	57	55
0,30	0	59	59

TABLE 6.1

.../TABLE 6.2

Motor speed rev./min.	Nett field current mA	Armature voltage volts	Armature current amps	Armature emf volts	$\frac{2p}{2a} Z_a \phi$ webers
754	10	7,2	0,216	3,5	0,280
760	20	9,1	0,125	7,0	0,552
749	30	11,1	0,106	9,3	0,744
751	40	13,2	0,103	11,4	0,912
760	50	14,7	0,103	12,9	1,016
755	60	16,0	0,105	14,2	1,128
750	70	16,8	0,107	15,0	1,200
748	80	17,4	0,109	15,6	1,248

(Armature resistance 17,14 ohms).

TABLE 6.2

Nett field current mA	Armatu - curr am	Torque newton metres	$\frac{2p}{2a} Z_a \phi$ webers
8	0,78	0,0218	0,176
16	0,78	0,0460	0,372
24	0,78	0,0666	0,[illegible]8
32	0,78	0,0828	0,660
40	0,78	0,0977	0,788

TABLE 6.3

Figure 6.1 shows nett field current plotted against amplifier input voltage, while figure 6.2 is a plot of the product $\frac{2p}{2a} Z_a \phi$ against nett field current for the motor. The effect of armature reaction upon the flux is apparent in this figure. The individual points plotted in figure 6.3 show the variation of $\frac{2p}{2a} Z_a \phi$ with input voltage when the amplifier is connected to the motor, while the curves are obtained from figure 2.4, being plotted so as to have the same initial slope and saturation value as the observed points. It can be seen that in this case a diode biasing voltage of 30 volts would have provided a reasonable fit to the observed data.

6.2 Capacitors

6.211 Capacitance

A Carey Foster bridge was used for the measurement of the capacitors used with the analogue computer.

Figure 6.4 shows the basic circuit of the bridge (no shielding arrangements are shown), balance being obtained by variation of M, Q, R and S. The balance equations are

$$C = \frac{M}{QR} \quad \text{and } L = M\left(1 + \frac{S}{Q}\right)$$

The bridge was calibrated against a standard capacitor. The shielding arrangements shown in figure 6.5 were used initially, and table 6.4 (sets one and two) shows the results obtained. It appears that stray capacitances of the order of 80 uuF existed. Set 3, table 6.4, shows the results of calibration measurements made with the shielding arrangements shown in figure 6.6; these shielding arrangements have reduced the stray capacitances to about 45 uuF.

.../TABLE 6.4

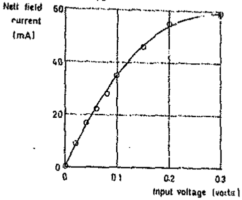

FIGURE 6·1

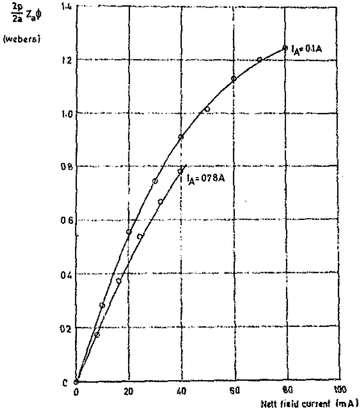

FIGURE 6·2

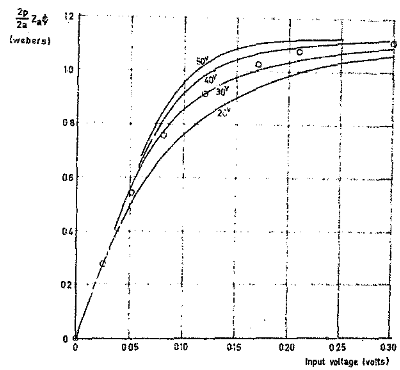

$\frac{2p}{2a} Z_a \phi$
(webers)
1.2
1.0
0.8
0.6
0.4
0.2
0
0
0.05
0.10
0.15
0.20
0.25
0.30
Input voltage (volts)
50V
40V
30V
20V

FIGURE 6-3

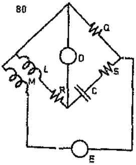

FIGURE 6.4

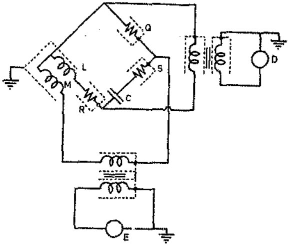

FIGURE 6.5

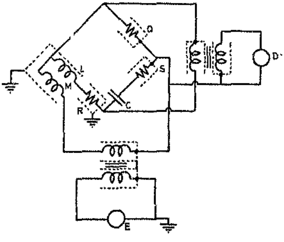

FIGURE 6.6

Set No.	Frequency Hz	Standard Capacitor uuF	Measured Capacitance uuF	Error uuF
1	500	500	578	78
		750	830	80
		1 000	1 081	81
	1 000	500	576	76
		750	827	77
		1 000	1 078	78
2	1 000	500	577	77
		750	828	78
		1 000	1 077	77
3	500	1 000	1 047	47
	600	1 000	1 046	46
	700	1 000	1 046	46
	800	1 000	1 045	45
	900	1 000	1 044	44
	1 000	1 000	1 043	43

TABLE 6.4

Table 6.5 gives the results of measurements on the polystyrene capacitors used with the analogue computer. Some of the capacitors were measured twice (set one and set two) and there appears to have been a uniform reduction of about 6 uuF in the values of the 0,01 uF capacitors and about 15 uuF in the values of the 0,1 uF capacitors. These reductions are most likely due to changes in the bridge and not in the capacitors, but as they were well within the expected accuracy of the bridge they were ignored.

.../ TABLE 6.5

Nominal Capacitance uF	Capacitor No.	Measured Capacitance Set 1 uF	Measured Capacitance Set 2 uF	Apparent change in Capacitance uuF
0,01	1	0,010025	0,010019	- 6
	2	0,009990	0,009984	- 6
	3	0,009881	0,009875	- 6
	4	0,010203	0,010199	- 4
	5	0,010171	0,010166	- 5
	6	0,009879	0,009872	- 7
	7	-	0,010114	-
	8	-	0,009989	-
	9	-	0,009932	-
	10	-	0,010075	-
0,03	1	-	0,030010	-
	2	-	0,030496	-
	3	-	0,029854	-
	4	-	0,029959	-
	5	-	0,031210	-
	6	-	0,030061	-
	7	-	0,031129	-
	8	-	0,029804	-
0,1	1	0,10026	0,10025	15
	2	0,10076	0,10074	15
	3	0,10133	0,10132	15
	4	0,10173	0,10170	29
	5	0,10097	0,10096	15
	6	0,09935	0,09934	14
	7	-	0,10011	-
	8	-	0,10130	-

TABLE 6.5

Some measurements were made to determine the sensitivity of the bridge, and table 6.6 shows the changes in component values necessary to cause a detectable unbalance in the bridge. The accuracy to which the values of the various components of the bridge were known results in an overall

.../accuracy

accuracy [illegible] 0,1%, and it can be seen that with the exception of the resista[illegible] (whose value is not required to calculate C) the sen[illegible] is at least an order of magnitude better than the accuracy.

	M		Q		R		S	
C uF	M uH	$\frac{\Delta M}{M}$ %	Q ohms	$\frac{\Delta Q}{Q}$ %	R ohms	$\frac{\Delta R}{R}$ %	S ohms	$\frac{\Delta S}{S}$ %
0,01	1	0,001	0,1	0,01	0,1	0,001	0,2	0,12
0,10	1	0,001	0,001	0,001	0,1	0,001	0,1	0,6

TABLE 6.6

6.212 Losses

The capacitor losses were obtained during measurements on a Schering bridge, and were found to be generally in agreement with values given in Table 2.1.

6.22 Resistors

The resistors used were high stability cracked carbon components ($\frac{1}{2}$ watt, $\pm$ 1%). Some initial tests were carried out on one resistor (0,1 megohm) to determine its temperature coefficient and dissipation constant. Table 6.7 gives the results obtained, and figures 6.7 and 6.8 show the variation of resistance with temperature (at constant power dissipation) and with power dissipation (at constant temperature). All resistance measurements were made with a four dial Wheatstone bridge, (accuracy 0,04%) and the resistor was always in still air. The ordinate in figures 6.7 and 6.8 is the ratio of the actual resistance

.../to

to its value when the resistor is in still air at 20°C with zero power dissipation. The temperature coefficient is – 310 p.p.m./°C, while the change in resistance due to power dissipation is 32 500 p.p.m./watt, leading to a dissipation constant of 9,54 mW/°C.

Ambient Temperature °C	Power Dissipa mW	Resistance megohms
19,0	100	0,10061
32,0	100	0,10022
36,0	100	0,10008
40,0	100	0,09992
45,0	100	0,09975
49,0	100	0,09974
51,0	100	0,09960
18,6	2	0,10097
18,6	3	0,10098
18,6	4	0,10096
18,6	9	0,10095
18,6	16	0,10092
18,6	25	0,10089
18,6	36	0,10085
18,6	49	0,10081
18,6	64	0,10076
18,6	81	0,10070
18,6	100	0,10064
18,6	121	0,10058
18,6	144	0,10050
18,6	169	0,10043
18,6	196	0,10035
18,6	225	0,10025

TABLE 6.7

.../ The

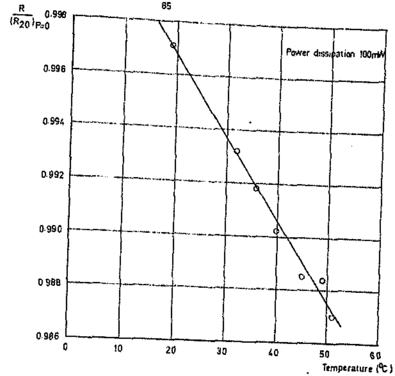

FIGURE 6·7

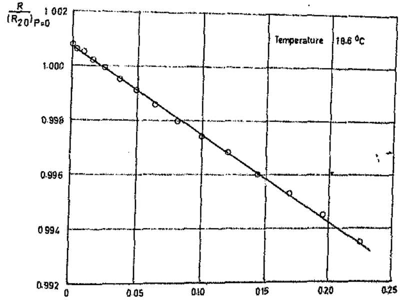

FIGURE 6·8

The full set of resistors used with the analogue computer were measured at temperatures of about 20°C and 60°C, and with power dissipations of 1 mW and 40 mW. Table 6.8 gives the resulting temperature coefficients and dissipation constants for these resistors, together with their resistance at 20°C and zero power dissipation. It can be seen that the 1 megohm resistors have both larger variations in temperature coefficient as well as a larger temperature coefficient, than the 0,1 megohm resistors. Dummer[32] has figures showing the properties of the carbon layer used in cracked carbon resistors which confirm this finding. The dissipation constants of both the 0,1 and 1 megohm resistors vary considerably, but it is not possible to state whether this was due to variations in the construction of the resistors or to variations in the heat transfer coefficient from the resistor to the air.

	Nominal Resistance value							
	0,1Megohm				1Megohm			
Res. No.	Res. at 20°C zero power megohms	Temp. coeff. α ppm/°C	Diss. const. B mW/°C	$\frac{\alpha}{B}$ ppm/mW	Res. at 20°C zero power megohms	Temp. coeff. α ppm/°C	Diss. const. B mW/°C	$\frac{\alpha}{B}$ ppm/mW
1	0,10092	-380	8,3	-46	1,0136	-480	7,8	-59
2	0,10029	-380	7,4	-51	1,0164	-460	7,7	-60
3	0,10091	-390	9,6	-41	1,0307	-670	11,9	-56
4	0,10011	-370	9,6	-39	1,0158	-460	9,5	-48
5	0,10076	-370	9,0	-41	1,0211	-670	9,0	-74
6	0,10052	-370	11,0	-34	1,0132	-440	7,1	-62
7	0,10000	-380	11,4	-33	1,0101	-440	7,5	-59
8	0,10058	-330	8,7	-44	1,0087	-540	8,7	-62
9	0,10055	-380	7,7	-49	1,0098	-400	7,4	-54
10	0,10032	-350	5,7	-61	1,0089	-450	8,0	-56
11	0,10089	-380	7,4	-51	1,0047	-370	7,7	-48
12	0,10055	-350	7,2	-49	1,0032	-330	6,8	-49
13	0,10024	-380	10,6	-36	1,0044	-370	6,3	-57
14	0,10008	-370	8,9	-42	1,0064	-300	7,3	-41
15	0,10047	-390	10,1	-39	0,9998	-360	7,0	-51

TABLE 6.8

.../6.23

6 The analogue circuit shown in figure 6.9 provides ar solution to the differential equation

The analogue circuit shown in figure 6.9 provides a solution to the differential equation

$$s^2v + w^2v = 0$$

This equation has a solution $v = A \sin (wt + \phi)$, A and ϕ being constants depending upon the initial conditions. The angular frequency w is given in terms of the component values of figure 6.9 by

$$w = \sqrt{\frac{R_f}{R_{in}\ R_1C_1R_2C_2}}$$

Thus the frequency can be calculated if component values are known, and conversely measurements of the frequency can be used to check measured component values.

Table 6.9 gives details of the component values used in a series of tests, together with both measured and calculated values of the period of oscillation. The accuracy of resistance measurement was $\pm$ 0,04%, and capacitors were measured to an accuracy of 0,1%, thus the maximum error in the period of oscillation would be expected to be about 0,18%. In all but one of the tests the discrepancy between observed and calculated periods is less than 0,18%, and the analogue circuit can be considered as operating satisfactorily and to have given results in accordance with those predicted from component values.

.../ TABLE 6.9

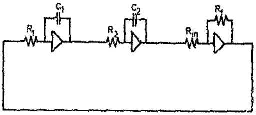

FIGURE 6-9

Test No.	R_1 MΩ	C_1 uF	R_2 MΩ	C_2 uF	R_{in} MΩ	R_f MΩ
1	0,5016	0,10076	0,4993	0,10026	1,0082	1,0062
2	0,5014	0,009990	0,4992	0,010171	1,0075	1,0057
3	1,0113	0,10060	1,0231	0,10157	0,10002	0,10063
4	1,0055	0,10025	0,09996	0,10074	0,10051	0,09978
5	1,0102	0,010025	1,0108	0,009990	1,0231	1,0106

Test No.	Measured Period ms	Calculated Period ms	Error	
			ms	%
1	316,14	316,36	-0,22	-0,07
2	31,736	31,717	+0,019	+0,06
3	645,10	644,03	+1,07	+0,17
4	63,364	63,536	-0,172	-0,27
5	63,930	63,931	-0,001	-0,002

TABLE 6.9

It is perhaps misleading to compare the difference between observed and calculated periods with a "maximum" expected error derived from the accuracies of the measurements of component values. This latter figure should more correctly be regarded as the average error which would result after a large number of observations. The scatter of individual observations about this average will depend upon the sensitivity of the equipment used for measuring both component values and the periods of oscillation. It is thus not impossible for individual values of the difference to exceed the "maximum" expected error. In view of the good agreement

.../between

between observed and calculated periods, this matter was not pursued.

6.3 Pen Recorder

The pen recorder was calibrated at different frequencies. The rms value of the applied voltage was measured with a vacuum tube voltmeter for frequencies higher than 20 Hz. At lower frequencies an oscilloscope calibrated against the vacuum tube voltmeter was used. Table 6.10 shows the results obtained, and figure 6.10 is a plot of the sensitivity (in dB with the d.c. value as reference) against frequency. It can be seen that the response is essentially flat from d.c. to about 50 Hz, where it is down by 3 dB.

Frequency Hz	Sensitivity			
	Left hand pen		Right hand pen	
	mm/volt	dB	mm/volt	dB
0	0,970	0	0,926	0
0,1	1,052	+0,70	0,990	+0,5[illegible]
0,3	0,997	+0,24	0,958	+0,29
1,0	0,983	+0,12	0,958	+0,29
3,0	0,972	+0,02	0,891	-0,34
10	0,947	-0,21	0,870	-0,54
20	0,965	-0,05	0,891	-0,34
30	0,954	-0,15	0,912	-0,14
40	0,909	-0,56	0,859	-0,65
50	0,784	-1,85	0,749	-1,84
60	0,611	-4,02	0,632	-3,32
80	0,417	-7,33	0,417	-6,93
100	0,254	-11,64	0,272	-10,64

TABLE 6.10

.../7.

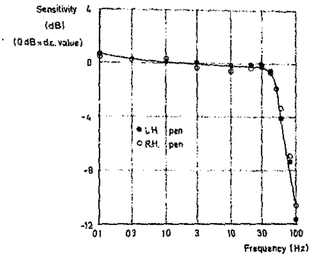

Sensitivity (dB)
(0 dB = d.c. value)
4
0
-4
-8
-12
● L.H. pen
○ R.H. pen
0.1
0.3
1.0
3
10
30
100
Frequency (Hz)

FIGURE 6-10

7. ACKNOWLEDGEMENTS

I should like to acknowledge the help and encouragement received from the following members of the staff of the Department of Electrical Engineering - Professor G.R. Bozzoli, Professor W. Cormack, Mr. G.J. Korvinek, Mr. D.Q. Mayne and Mr. K. Posel.